The Journal of Immunology

Bcl6 Expressing Follicular Helper CD4 T Cells Are Fate Committed Early and Have the Capacity To Form Memory

Youn Soo Choi, Jessica A. Yang, Isharat Yusuf, Robert J. Johnston, Jason Greenbaum, Bjoern Peters and Shane Crotty

J Immunol 2013; 190:4014-4026; Prepublished online 13 March 2013;
doi: 10.4049/jimmunol.1202963
http://www.jimmunol.org/content/190/8/4014

The Journal of Immunology is published twice each month by
The American Association of Immunologists, Inc.,
1451 Rockville Pike, Suite 650, Rockville, MD 20852

Print ISSN: 0022-1767 Online ISSN: 1550-6606.

Bcl6 Expressing Follicular Helper CD4 T Cells Are Fate Committed Early and Have the Capacity To Form Memory

Youn Soo Choi,* Jessica A. Yang,* Isharat Yusuf,* Robert J. Johnston,*,† Jason Greenbaum,* Bjoern Peters,* and Shane Crotty*,†,‡

Follicular helper CD4 T (Tfh) cells are a distinct type of differentiated CD4 T cells uniquely specialized for B cell help. In this study, we examined Tfh cell fate commitment, including distinguishing features of Tfh versus Th1 proliferation and survival. Using cell transfer approaches at early time points after an acute viral infection, we demonstrate that early Tfh cells and Th1 cells are already strongly cell fate committed by day 3. Nevertheless, Tfh cell proliferation was tightly regulated in a TCR-dependent manner. The Tfh cells still depend on extrinsic cell fate cues from B cells in their physiological in vivo environment. Unexpectedly, we found that Tfh cells share a number of phenotypic parallels with memory precursor CD8 T cells, including selective upregulation of IL-7Rα and a collection of coregulated genes. As a consequence, the early Tfh cells can progress to robustly form memory cells. These data support the hypothesis that CD4 and CD8 T cells share core aspects of a memory cell precursor gene expression program involving Bcl6, and a strong relationship exists between Tfh cells and memory CD4 T cell development. ***The Journal of Immunology*****, 2013, 190: 4014–4026.**

Follicular helper CD4 T (Tfh) cells are a subset of differentiated CD4 T cells that express CXCR5, the chemokine receptor for B cell homing chemokine CXCL13 (1). Surface CXCR5 expression enables Tfh cells to migrate into B cell follicles, where they provide help to B cells to form germinal centers (2). Tfh cells are required for generation of long-lived plasma cells and memory B cells through cognate interactions with germinal center B cells as well as production of B cell help cytokines such as IL-21 (3). Differentiation of effector CD4 T cell subsets is controlled by specific transcription factors (1, 4), and CD4 T cell differentiation into Tfh cells is regulated by the transcription factor Bcl6 (1). *Bcl6*-deficient CD4 T cells fail to differentiate into Tfh cells (5–7), whereas constitutive expression of Bcl6 instructs murine and human CD4 T cells to differentiate into Tfh cells (6, 8).

Because of the importance of Bcl6 in Tfh cell differentiation, regulation of Bcl6 in CD4 T cells is of substantial interest. Several recent studies, including our own work, demonstrated that Bcl6 protein induction occurs quite early after CD4 T cells receive activation signals both in vivo (9–11) and in vitro (12–14). During the dendritic cell (DC) priming stage of CD4 T cells, ICOS is a key upstream molecule for induction of Bcl6 (9). In contrast, high expression of IL-2Rα and IL-2–dependent signaling through STAT5 severely limits Tfh differentiation (15). Tfh differentiation is augmented by reduced IL-2Rα gene copy number (IL-2Rα$^{+/-}$) or curtailed by exogenous IL-2 treatment (15, 16). Initial Bcl6 induction and subsequent CXCR5 expression leads CD4 T cells to the B–T border, where Tfh cells interact with cognate B cells to maintain Bcl6 expression for full differentiation and maintenance of the Tfh phenotype (1, 9, 11, 17).

Cells with Tfh and non-Tfh phenotypes are distinguishable from very early time points in vivo (9–11, 18). However, whether the early pathways for development of Tfh versus non-Tfh cells would be maintained in a given immune response remains an open issue. Very recently, Dong and colleagues (19) reported that Tfh and Th2 cells remain their original phenotypes in recipient mice after rechallenge with Ag, indicating Tfh versus non-Tfh differentiation pathways are stable but not interconvertible. However, an earlier report demonstrated that Tfh cells can develop from IL-4–producing CXCR5$^-$ CD4 T cells in recipient mice after Ag challenge (20). Indeed, it is well established from plasticity studies that many types of differentiated CD4 T cells can lose their differentiation program and acquire new differentiation programs (4, 12, 21–23). A recent study provided evidence of potential plasticity of Tfh cells in part by analysis of epigenetic modifications, which revealed positive regulatory H3K4me3 marks on major transcriptional regulators of Th1 (*Tbx21*), Th2 (*Gata3*), and Th17 (*Rorc*) cells, in ex vivo– and in vitro–generated Tfh cells (12). Furthermore, there are molecules capable of regulating both Tfh and Th1 cells. IL-12–mediated STAT4 activation has been associated with Bcl6 induction in CD4 T cells during Th1 differentiation, which presents a potential mechanism for plasticity between Tfh and Th1 cell differentiation (13, 14). Unexpectedly, excessive IFN-γ signaling augments Tfh differentiation in Sanroque mice, driving autoantibody responses (24).

The transcriptional regulator Blimp1 is also involved in CD4 T cell differentiation and is a key negative regulator of Tfh differentiation (6, 15). Through reciprocal regulations of Bcl6 and Blimp1, Tfh cell differentiation is distinguished from CD4 T cell

*Division of Vaccine Discovery, La Jolla Institute for Allergy and Immunology, La Jolla, CA 92037; †Department of Medicine, University of California, San Diego School of Medicine, La Jolla, CA 92037; and ‡Center for HIV/AIDS Vaccine Immunology and Immunogen Discovery, La Jolla, CA 92037

Received for publication October 25, 2012. Accepted for publication February 11, 2013.

This work was supported by National Institutes of Health, National Institute of Allergy and Infectious Diseases Grants R01 072543 and R01 063107, The Scripps Research Institute Center for HIV/AIDS Vaccine Immunology and Immunogen Discovery Award UM1AI100663, and La Jolla Institute for Allergy and Immunology institutional funds (to S.C.).

Address correspondence and reprint requests to Dr. Shane Crotty, La Jolla Institute for Allergy and Immunology, 9420 Athena Circle, La Jolla, CA 92037. E-mail address: shane@liai.org

The online version of this article contains supplemental material.

Abbreviations used in this article: B6, C57BL/6J; BTLA, B and T lymphocyte attenuator; DC, dendritic cell; KLH, keyhole limpet hemocyanin; LCMV, lymphocytic choriomeningitis virus; NP-OVA, 4-hydroxy-3-nitrophenyl acetyl-OVA; PSGL1, P-selectin glycoprotein ligand 1; SLAM, signaling lymphocyte activation molecule; Tfh, follicular helper CD4 T.

www.jimmunol.org/cgi/doi/10.4049/jimmunol.1202963

differentiation into other differentiated cell types (Th1, Th2, Th17, and induced regulatory T cells) (1, 6, 25, 26). Bcl6 can repress Blimp1 expression by directly binding to the *Prdm1* gene (encoding Blimp1) (27, 28). In B cells, Bcl6 is critically required for germinal center B cell differentiation and survival, whereas Blimp1 drives terminal differentiation of B cells into plasma cells (29, 30). Antagonistic regulation of Bcl6 and Blimp1 is also associated with molecular regulation of fate determination of CD8 T cells (31, 32). Recent studies demonstrated Tfh cells contribute to memory compartment of CD4 T cells (18, 19, 33). We therefore explored the regulation of Bcl6 and the stability of Tfh cell differentiation and the potential relationship between Bcl6 expression of Tfh cells and memory CD4 T cell formation.

Using adoptive cell transfer experiments, we found that early $Bcl6^+CXCR5^+$ Tfh cells exhibited substantial cell fate commitment and B cell help capacities. Gene expression profile analysis revealed that mature Tfh cells and early memory precursor CD8 T cells share a transcriptional signature, including Bcl6 expression and IL-7Rα re-expression. We demonstrate that Tfh cells contribute substantially to memory CD4 T cell generation after a viral infection, implying that aspects of Tfh differentiation and memory CD4 T cell development have shared mechanisms.

Materials and Methods

Mice and viral infections

C57BL/6J (B6), B cell-deficient μMT (B6 μ*MT*), and TCRα-deficient (B6.129S2-*Tcra*^{tm1Mom}/J) mice were purchased from The Jackson Laboratory. SMARTA ('SM'. LCMV gp66-77-IA^b specific) (34) and Blimp1-YFP BAC tg mice (35) were obtained from in-house breeders at LIAI. Lymphocytic choriomeningitis virus (LCMV) Armstrong strain was made, and PFUs were determined as described previously (36). All animal experiments were performed in compliance with approved animal protocols at LIAI. Whole-genome microsatellite analysis was conducted through the UCLA Southern California Genotyping Consortium. SM mice were >99% B6.SJL *Ptprc*^{a}. All mice were housed in ventilated racks with HEPA filters and provided with irradiated PicoLab Rodent Diet (20-5053) food.

4-Hydroxy-3-nitrophenyl acetyl-OVA and gp61-keyhole limpet hemocyanin immunization

4-Hydroxy-3-nitrophenyl acetyl-OVA (NP-OVA) was prepared in alum and injected as described previously (6). Briefly, three parts of NP_{19}-OVA (Biosearch Technologies) in PBS were mixed with one part of Alum (Pierce) for 60 min at 4°C. A total of 100 μg NP-OVA-Alum immunizations were done i.p. gp61-keyhole limpet hemocyanin (KLH) was prepared as follows. LCMV gp61 peptide (GLNGPDIYKGVYQFKSVEFD) was conjugated to malemide-activated KLH following the manufacturer's protocol (Pierce). A total of 20 μg gp61-KLH was resuspended in alum with 2 μg LPS for i.p. injections.

Retrovirus production and CD4 T cell transduction

Blimp1-expressing retroviral vector (pMIG-GFP) or empty vector (GFP only) was used to produce virions from the Plat-E cell line as described previously (6). Culture supernatants were obtained 2 d after transfections and filtered through 0.45-μm syringe filters. CD4 T cells were negatively isolated by using CD4 T cell isolation kit (Miltenyi Biotec) for retroviral transductions as described previously (6). Briefly, cells were in vitro stimulated with 8 μg/ml anti-CD3 (clone 17A2; BioXCell) and anti-CD28 (clone 37.51; BioXCell) and then transduced with retroviral virions 24 and 36 h poststimulation. Transduced CD4 T cells were FACS sorted based on GFP expression levels.

Flow cytometry

Single-cell suspensions were obtained by a gentle mechanical disruption of spleens, followed by ACK lysis buffer to remove RBCs. Cell suspensions were stained with the following mAbs in FACS buffer (PBS with 0.5% BSA): CD4, CD8, Bcl6, CXCR5, PSGL-1, and pSTAT5 (BD Biosciences); signaling lymphocyte activation molecule (SLAM) (CD150, BioLegend); and CD200, CD44, CD45.1/2, IL-2Rα (CD25), IL-7Rα (CD127), L-selectin, CD69, B220, Ly-6C, B and T lymphocyte attenuator (BTLA), and IFN-γ (eBioscience).

CXCR5 stains were performed as described previously (6, 9). For early time point analysis (days 2 and 3 after LCMV infection), biotinylated CXCR5 (BD Biosciences) was used. Briefly, cells were stained with biotinylated CXCR5 mAb in FACS buffer for 30 min at 4°C, washed with FACS buffer twice, followed by secondary step stains with streptavidin–PE (PE Cy7 or allophycocyanin) (eBioscience) and mAbs for other surface molecules of interest. For later time point analysis, the tertiary CXCR5 stain was used. Briefly, cells were stained with purified anti-CXCR5 mAb (BD Biosciences) for 1 h at 4°C, washed with FACS buffer twice, and stained with secondary biotinylated goat anti-rat Ig(H+L) (Jackson ImmunoResearch Laboratories) for 30 min at 4°C. After two washes with FACS buffer, tertiary staining was performed with streptavidin–PE (PE Cy7 or allophycocyanin) (eBioscience) and other mAbs for surface molecules of interest. Primary and secondary stains were done in PBS + 0.5% BSA + 2% FCS + 2% normal mouse serum.

Intracellular Bcl6 (K112-91) was performed using Foxp3 staining buffers (eBioscience). The cells were fixed (30 min to 1 h) at 4°C and then washed twice with 1× permeabilization buffer. Anti-Bcl6 mAbs were diluted in 1× permeabilization buffer and applied to fixed samples (30 min to 1 h) at 4°C.

For intracellular IFN-γ stain, splenocytes were stimulated with PMA (20 ng/ml) and ionomycin (1 μM) for 4 h in the presence of brefeldin A. Intracellular IFN-γ was detected as described previously (6).

All FACS samples were washed twice with FACS buffer and either acquired using an LSRII (BD Biosciences) or sorted by FACS Aria (BD Biosciences). Data were analyzed using FlowJo (Tree Star).

CellTrace Violet label

Cell suspensions were washed and resuspended in PBS at 10^7 cells/ml concentration. CellTrace Violet (Invitrogen) at a final concentration of 2.5 μM was incubated with cells for 20 min at 37°C, protected from light. Unlabeled CellTrace Violet was then quenched by adding two to five times volume of FBS to the original staining volume of cell suspensions, spun, and resuspended in appropriate media.

Cell transfer and in vitro culture

Naive SM CD4 T cells were purified from whole splenocytes by negative selection using magnetic beads (Miltenyi Biotec). Naive SM or retrovirally transduced OVA 323-339 I-A^b (OTII) CD4 T cells were transferred into recipient mice by i.v. injections via the retro-orbital sinus. Cell transfer numbers for each time point were as follows: for naive SM cells, 1×10^6, $4–5 \times 10^5$, and 5×10^3 SM $CD4^+$ T cells for day 2, 3, and 8 experiments, respectively. A total of 2.5×10^3 transduced OTII CD4 T cells were transferred for analysis of OTII CD4 T cells 8 d after NP-OVA protein immunization. For adoptive transfers of sorted cells in the fate commitment and memory analysis, two groups of infection-matched B6 or $TCR\alpha^{-/-}$ mice were injected with the same numbers of Tfh and Th1 SM cells (range of $50–100 \times 10^3$). DMEM was used for all adoptive cell transfer procedure.

For in vitro cultures of Tfh and Th1 SM cells, 96-well flat bottom plates were precoated with 8 μg/ml anti-CD3 and anti-CD28, unless the amount of anti-CD28 mAb was specified in the figure legends. Cells were resuspended in the complete culture media (DMEM + 10% FCS supplemented with 2 mM GlutaMAX [Life Technologies], 100 U/ml penicillin/streptomycin [Life Technologies], and 50 μM β-mercaptoethanol) and 2 ng/ml recombinant human IL-7 (PeproTech).

Microarray meta-analysis

Datasets. All CEL files were downloaded from the National Center for Biotechnology Information Gene Expression Omnibus database (GSE19825 and GSE21379–GSE21381).

Data normalization and summarization. Data from three separate studies were analyzed in this analysis. Microarrays were background-corrected and normalized using the "rma" function of the Bioconductor "affy" package (37). Data from each study were normalized separately. Within each study, each possible comparison of Th1 versus Tfh and CD8 effector versus CD8 memory precursors was performed. Genes that had an average 2-fold difference across all comparisons are included in Supplemental Table I. A heat map for selected genes of interest was generated using matrix2png (38) and shown in Fig. 5B.

Statistics

Statistical analyses were done using Prism 5.0 (GraphPad), and *p* values were obtained by using two-tailed unpaired Student *t* tests with a 95% confidence interval. Error bars on bar graphs depict the SEM. For statistical analysis of microarray data, a contingency table of genes that were up- or downregulated in both the Th1 versus Tfh CD4 T cells and effector versus memory pre-

cursors CD8 T cells comparisons was produced (Supplemental Table I) and used to calculate $p = 1.0 \times 10^{-14}$ with a Fisher's exact test.

Results

Early Tfh versus Th1 bifurcation after acute viral infection

Bcl6$^+$CXCR5$^+$ Tfh cells are generated early during the DC priming stage of immune responses (9–11, 39). Careful analysis of Bcl6 protein expression during the early phase of CD4 T cell activation confirmed that Bcl6 is specifically induced early in Tfh cells (Fig. 1A, 1B, Supplemental Fig. 1). At the same time points after LCMV infection, Bcl6$^-$CXCR5$^-$ non-Tfh cells are also identifiable and were shown to strongly express IL-2Rα, the high-affinity IL-2R subunit, and Blimp1, as measured with a Blimp1-YFP reporter (9, 18). We then established that the non-Tfh SM cells were Th1 cells. Day 3 IL-2Rα$^+$Blimp1$_{YFP}^+$ non-Tfh and IL-2Rα$^-$Blimp1$_{YFP}^-$ Tfh cells were sorted for quantitative PCR analysis. *Tbx21* mRNA (encoding T-bet) was expressed 10-fold higher in IL-2Rα$^+$Blimp1$_{YFP}^+$ cells compared with IL-2Rα$^-$Blimp1$_{YFP}^-$ Tfh cells ($p = 2.5 \times 10^{-6}$; Fig. 1C). T-bet protein was strongly expressed in IL-2Rα$^+$Blimp1$_{YFP}^+$ cells ($p = 0.0004$; Fig. 1D). IL-2Rα$^+$ cells were the major population in IFN-γ production at day 3 after LCMV infection ($p = 2.3 \times 10^{-5}$; Fig. 1E). Thus, the early Tfh cells are CXCR5$^+$IL-2Rα$^{int/-}$Blimp1$_{YFP}^-$, and the T-bet^{hi}IL-2Rα$^+$Blimp1$_{YFP}^+$ cells are Th1 cells.

Cell fate commitment of early Tfh and Th1 cells

Different models have been put forward as to whether Tfh differentiation is an independent pathway or a subsequent state of other effector CD4 T cells (1, 9, 40). Therefore, we explored whether early Bcl6$^+$CXCR5$^+$ CD4 T cells are cell fate committed. To address whether early Tfh and Th1 cells interconvert, we sorted Tfh and Th1 cells from "donor" B6 mice 3 d after LCMV infection for transfers into recipient mice (Fig. 2A). SM cells were sorted as either IL-2Rα$^+$Blimp1$_{YFP}^+$ (Bcl6$^-$CXCR5$^-$) Th1 cells or IL-2Rα$^-$Blimp1$_{YFP}^-$ (Bcl6$^+$CXCR5$^+$) Tfh cells (Fig. 2A–C) and then transferred into separate groups of infection-matched B6 recipients to provide the same physiological environment (Fig. 2A). Eight days after LCMV infection (5 d after transfers), we examined Tfh and Th1 cell–recipient mice to analyze the stability of Tfh and Th1 cell populations in each recipient group. Quite strikingly, we found that Tfh and Th1 cells maintained their original phenotypes (Fig. 2D). The vast majority of input Tfh cells remained SLAM^{lo}CXCR5$^+$ Tfh cells (80–92%, $p = 2.7 \times 10^{-10}$; Fig. 2D, 2E). The majority of input Th1 cells retained their phenotype and did not convert to Tfh cells (80–87%, $p = 1.4 \times 10^{-9}$; Fig. 2D, 2E). High levels of Bcl6 were maintained by transferred Tfh SM cells ($p = 5.9 \times 10^{-6}$; Fig. 2F), whereas Blimp1$_{YFP}$ was highly expressed by SM cells in Th1 recipients B6 mice ($p = 3.7 \times 10^{-10}$; Fig. 2G). Tfh cells are distinguished from other effector CD4 T cells, by their prominent roles in providing B cell help (1). Hence, we addressed whether day 3 Tfh cells were capable of B cell help. Day 3 Tfh and Th1 cells were isolated from LCMV infected donor B6 mice and then transferred into TCRα$^{-/-}$ mice that were immunized with gp61-KLH. Day 3 Tfh cells were able to induce germinal center B cells in TCRα$^{-/-}$ mice ($p = 2.7 \times 10^{-3}$; Fig. 2H), which was associated with a robust formation of

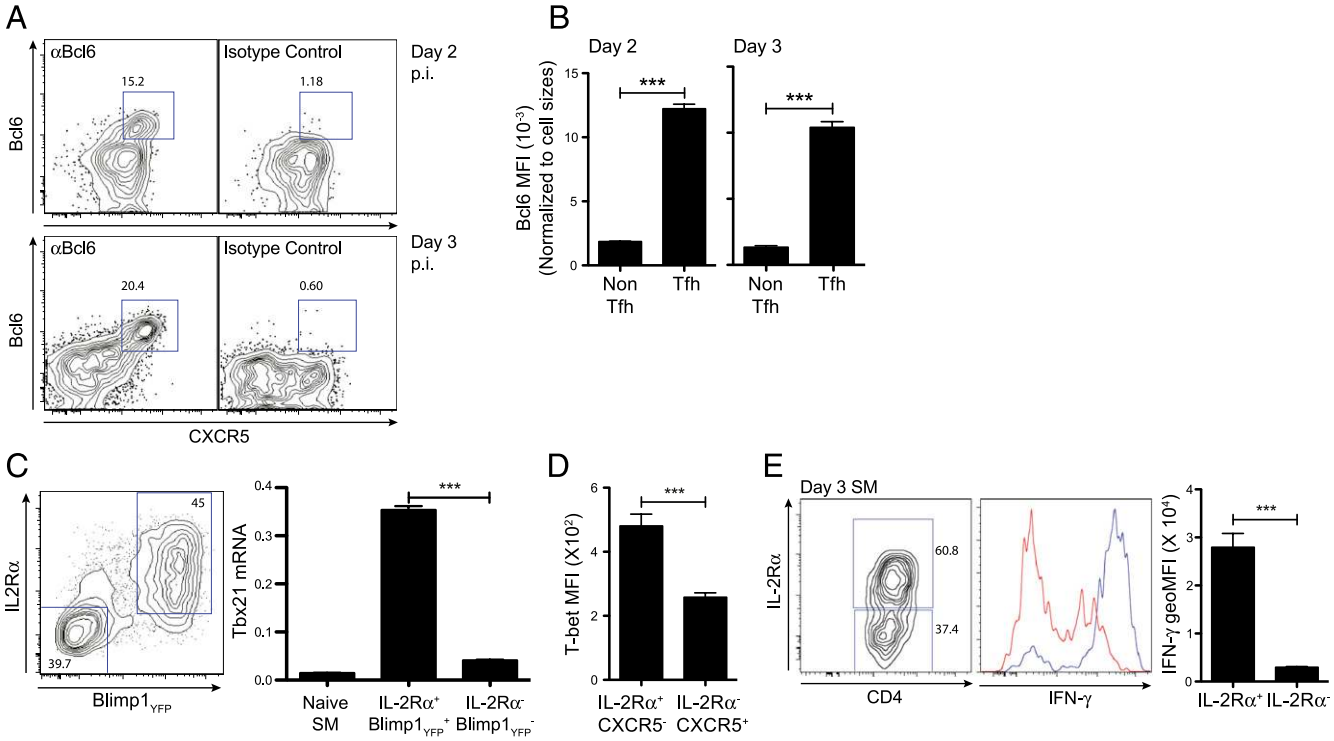

FIGURE 1. Early bifurcation of Tfh and Th1 differentiation pathway occurs after an acute viral infection. (**A** and **B**) Analysis for Bcl6 expression by SM CD4 T cells after LCMV infection. (A) Isotype control stains were included to gate Bcl6$^+$ SM cells of 2-d (*upper panels*) and 3-d (*lower panels*) LCMV-infected mice. (B) Bcl6 expression levels calculated by normalization of Bcl6 mean fluorescence intensities (MFIs) of Tfh versus non-Tfh SM cells by cell sizes. (**C**) Naive Blimp1-YFP SM (CD45.1$^+$) cells were transferred into B6 mice, from which IL-2Rα$^+$Blimp1$_{YFP}^+$ non-Tfh and IL-2Rα$^-$Blimp1$_{YFP}^-$ Tfh cells were sorted at day 3 after LCMV infection. Quantitative PCR was conducted to measure *Tbx21* mRNA. Quantification made by fold induction of *Tbx21* over *Gapdh*. (**D** and **E**) Naive SM (CD45.1$^+$) CD4 T cells were transferred into B6 (CD45.2$^+$) mice that were subsequently infected with LCMV. (D) T-bet MFIs calculated for IL-2Rα$^+$CXCR5$^-$ and IL-2Rα$^-$CXCR5$^+$ SM cells. (E) IFN-γ intracellular cytokine stains conducted to detect IFN-γ production after PMA/ionomycin stimulation. SM cells were gated based on IL-2Rα expression (*left panel*). Overlaid histograms of IFN-γ of IL-2Rα$^+$ non-Tfh (blue) and IL-2Rα$^-$ (red) Tfh SM cells (*middle panel*). Quantification made by geometric MFI of IFN-γ (*right panel*). Data are representative of two independent experiments using four to five mice per group (A, B, D, E) and triplicate wells (C) per sample. ***$p < 0.001$, shown as mean and SEM.

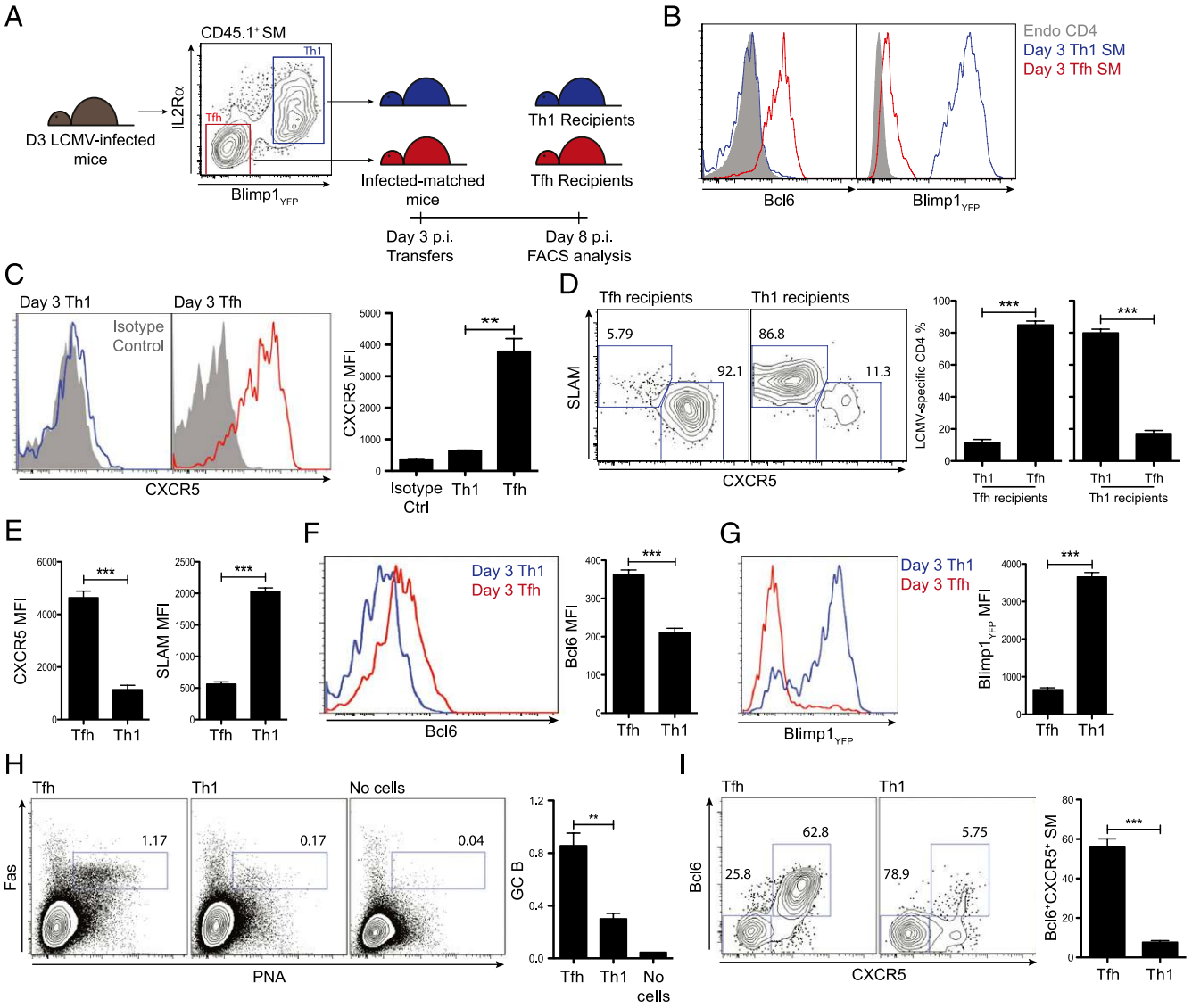

FIGURE 2. Tfh cells are fate determined early during an acute viral infection. (**A**–**G**) Naive Blimp1-YFP SM (CD45.1$^+$) CD4 T cells were transferred into B6 (CD45.2$^+$) mice that were infected with LCMV. (A) Three days after LMCV infection, SM cells were FACS sorted into Tfh (IL-2Rα$^-$Blimp1$_{YFP}^-$) versus Th1 (IL-2Rα$^+$Blimp1$_{YFP}^+$) SM cells. The sorted Tfh and Th1 SM cells were transferred into separate groups of infection-matched B6 mice and analyzed 5 d later. (B) Overlaid histograms for Bcl6 (*left panel*) and Blimp1$_{YFP}$ (*right panel*) by day 3 Th1 (blue) and Tfh (red) SM cells, with endogenous CD4 T cells (gray filled). (C) Overlaid histograms for CXCR5 expression by day 3 Th1 (blue) and Tfh (red) SM cells. Gray-filled histograms show background stains by isotype control (rat IgG2a) mAb. Quantitation calculated as mean fluorescence intensities (MFIs). (D) Representative FACS plots of splenic SM cells in Tfh (*left*)- and Th1 (*right*)-recipient mice 5 d after transfer. Gates indicate Th1 (SLAM^{hi}CXCR5^{lo}) and Tfh (SLAM^{lo}CXCR5^{hi}) SM cells. Relative frequencies of Th1 and Tfh SM cells calculated as percentages of respective populations among total SM cells in Th1- and Tfh-recipient mice. (E) MFIs of CXCR5 and SLAM were calculated on total SM cells in Th1- and Tfh-transferred mice. Overlaid histograms of Bcl6 (F) and Blimp1$_{YFP}$ (G) expressions by SM cells in Th1 (blue)- and Tfh (red)-recipient mice. MFIs were calculated. (**H** and **I**) Day 3 Tfh and Th1 cells were isolated as shown in Fig. 2A and were transferred into TCRα$^{-/-}$ mice that had been immunized with gp61-KLH 48 h prior to adoptive cell transfer. The mice were analyzed 10 d after immunization. (H) Shown are representative FACS plots of germinal center B cells (Fas$^+$PNA$^+$) of Tfh, Th1, or no cell-transferred TCRα$^{-/-}$ splenocytes. Quantitation calculated as percentage of germinal center B cells among total B cells. (I) Representative FACS plots of donor cells. Gates indicate Bcl6$^+$CXCR5$^+$ Tfh cells. Percentage of Tfh cells among total donor cells. Data are representative of two independent experiments using five to six mice per group. $^{**}p < 0.01$, $^{***}p < 0.001$, shown as mean and SEM.

Bcl6$^+$CXCR5$^+$ Tfh cells ($p = 1.0 \times 10^{-5}$; Fig. 2I). These results demonstrate that Tfh and Th1 cells are predominantly fate committed within 72 h of responding to an acute infection, both by transcription factor expression and cell function.

Early Tfh cells require Ag presentation for every round of cell division

When we analyzed Tfh and Th1 cell–recipient B6 mice, we observed that SM cell recoveries from Tfh cell recipients were 5- to 10-fold more than from Th1 cell recipients ($p = 6.3 \times 10^{-5}$; Fig. 3A). Comparable levels of activation of endogenous CD4 and CD8 T cells excluded the possibility of different levels of LCMV infection (data not shown). We therefore examined whether early Tfh cells have different proliferative capacity than Th1 cells. To address this point, Tfh cells (IL-2Rα$^-$Blimp1$_{YFP}^-$) and Th1 cells (IL-2Rα$^+$Blimp1$_{YFP}^+$) were sorted from B6 mice 3 d after LCMV infection as described in Fig. 2A, labeled with a proliferation tracking dye, and then transferred into infection-matched B6 mice.

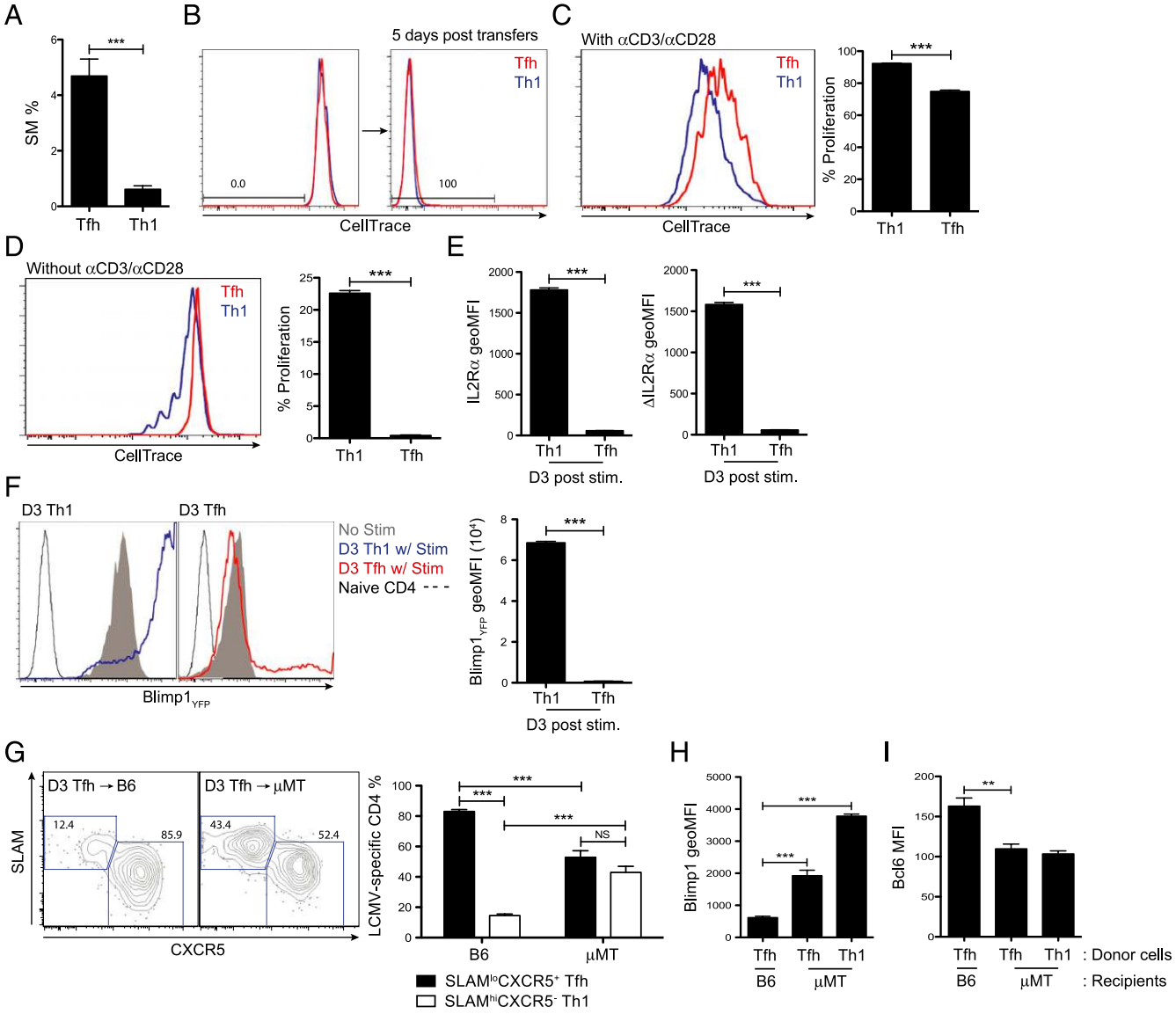

FIGURE 3. Fate-committed Tfh cells require continuous antigenic stimulation to proliferate. (**A**) SM CD4 T cell expansion (percentage of total CD4 T cells) in the spleens of Tfh versus Th1 cell recipient mice (shown in Fig. 2). (**B**) Day 3 Tfh and Th1 cells were sorted (Fig. 2A), labeled with CellTrace Violet, and then transferred into infection-matched mice. Overlaid histograms show CellTrace Violet in Th1 (blue) and Tfh (red) cells before (*left panel*) and 5 d after (*right panel*) cell transfer. (**C**–**F**) Three days after LCMV infection, SM Tfh and Th1 cells were sorted, CellTrace Violet labeled, and then cultured for 3 d in vitro. Overlaid histograms of CellTrace Violet labeled Th1 (blue) and Tfh (red) cells 3 d after in vitro culture with (C) or without (D) anti-CD3/28 mAbs. (E) IL-2Rα levels calculated as geometric mean fluorescence intensities (MFIs) (*left panel*) and by ΔIL-2Rα geometric MFIs (*right panel*, IL-2Rα $geoMFI_{w/\ stim}$ − IL-2Rα $geoMFI_{w/o\ stim}$). (F) Overlaid histograms for $Blimp1_{YFP}$ expressions by ex vivo Th1 (blue) and Tfh (red) SM cells following anti-CD3/28 stimulation. Calculated as geometric MFIs. Gray-filled histograms show $Blimp1_{YFP}$ levels by Th1 and Tfh cells cultured in the absence of stimulation. (**G**–**I**) $Bcl6^+CXCR5^+$ Tfh ($CD45.1^+$) cells were obtained from day 3 LCMV–infected B6 mice, transferred into infection-matched B6 or B cell–deficient μMT-recipient ($CD45.2^+$) mice, and analyzed 5 d after transfers. (G) Representative FACS plots of transferred ($CD45.1^+$) cells. Gates indicate Th1 ($SLAM^{hi}CXCR5^-$) and Tfh ($SLAM^{lo}CXCR5^+$) cells. Relative frequencies of Th1 and Tfh populations calculated as percentage of total transferred cells. Levels of $Blimp1_{YFP}$ (H) and Bcl6 (I) expression by transferred cells in Tfh-recipient B6 and μMT mice and Th1-recipient μMT mice. Data are representative of two or more independent experiments using five to six mice (A, B, G–I) and three to four replicate wells (C–F) per group. $^{**}p < 0.01$, $^{***}p < 0.001$, shown as mean and SEM.

Five days after transfers, both Tfh and Th1 cells had fully diluted the proliferation tracking dye (Fig. 3B), which indicated that both cell types proliferated extensively (≥10 divisions).

We next investigated the proliferation capacities of Tfh and Th1 cells in a defined in vitro environment. For this, Tfh and Th1 SM cells were sorted from LCMV infected mice 3 d postinfection (Fig. 2A) and cultured in the presence or absence of TCR- and co-stimulation-mediated activation (anti-CD3/CD28 mAbs) (Fig. 3C, 3D). In the presence of stimulation, Th1 cells proliferated more than Tfh cells ($p = 6.3 \times 10^{-6}$; Fig. 3C). Interestingly, we also found that Th1 cells underwent several rounds of cell division in the absence of antigenic stimulation, which was in marked contrast to Tfh cells that underwent no proliferation in the absence of TCR-mediated stimulation ($p = 5.9 \times 10^{-6}$; Fig. 3D).

TCR stimulation leads to upregulation of IL-2Rα on T cells (41). This results in a possible conundrum during the expansion phase of the CD4 T cell response, where repeated TCR stimulation is strictly required for Tfh cell proliferation but also results in antagonism of Bcl6 by upregulation of IL-2Rα and Blimp1 (9, 15). We therefore examined the regulation of these proteins in early Tfh

and Th1 cells during proliferation. Day 3 Tfh cells do not express IL-2Rα or Blimp1$_{YFP}$ (Fig. 3E, 3F), but Tfh cells nevertheless require TCR stimulation for continued expansion. Interestingly, TCR stimulation of Tfh cells did not induce IL-2Rα expression in contrast to robust upregulation of IL-2Rα on Th1 cells in vitro after TCR stimulation ($p = 7.6 \times 10^{-11}$; Fig. 3E, *right panel*). We infer that avoidance of IL-2Rα induction is important for Tfh cell maintenance, because upregulation of IL-2Rα on Th1 cells after TCR stimulation was associated with a 10-fold further induction of Blimp1$_{YFP}$ (Fig. 3F). Therefore, proliferating Tfh cells dissociate TCR signaling from IL-2Rα expression.

A series of studies has demonstrated that Ag presentation first by DCs during the CD4 T cell priming stage followed by Ag presentation by B cells is a prerequisite for CD4 T cells to initiate and then complete Tfh differentiation (2, 6, 9, 42–45). The strict Ag dependence of Tfh cell proliferation made us investigate whether Ag presentation in vivo may affect cell fate commitment in Tfh cells. For this, fate-committed Tfh cells were sorted from LCMV-infected mice at day 3 postinfection and transferred into infection-matched B6 and B cell–deficient μMT mice. Within the normal physiological environment (B6 mice), fate-committed Tfh cells (Bcl6$^+$CXCR5$^+$) again maintained their phenotype as Tfh cells (Fig. 3G). However, transferred Tfh cells were lost in the absence of B cells. Indeed, in Tfh cell–recipient μMT mice, Blimp1$_{YFP}^-$ expressing Th1 cells (SLAM^{hi}CXCR5$^-$) were highly enriched 5 d after cell transfers (15 ± 2% in B6 versus 43 ± 8% in μMT) (Fig. 3G, 3H). Our data indicate that B cells are important APCs for Tfh cells not only for maintenance of Bcl6 expression (Fig. 3I) (9) but also for each round of cell proliferation (Fig. 3D).

Fate-committed Tfh cells share a molecular signature with CD8 T memory precursors

Our data indicate that the fate-committed differentiation of early bifurcated Tfh versus Th1 cells is strongly associated with reciprocal regulation of Bcl6 and Blimp1. Interestingly, antagonistic Bcl6–Blimp1 signaling axis is also observed during the Ag-specific CD8 T cell differentiation; Bcl6$^+$ memory precursor CD8 T cells and Blimp1$^+$ short-lived effector CD8 T cells are present at the peak response to LCMV infection (46). The gene expression pattern of these two CD8 T cell populations has been characterized (35). Memory precursor CD8 T cells express elevated levels of Bcl6, whereas terminal effector CD8 T cells express elevated levels of Blimp1, which led us to investigate whether Bcl6-expressing Tfh versus Blimp1$^+$ Th1 cells may possess similar molecular regulation to memory precursor versus effector precursor CD8 T cells. Given that memory precursor CD4 T cells were recently proposed to be present in a PSGL1^{hi}Ly6C^{lo} population (47), we examined whether Bcl6- and Blimp1-based phenotyping is recapitulated by phenotypic analysis of CD4 T cells based on P-selectin glycoprotein ligand 1 (PSGL1) and Ly6C. At day 8 after LCMV infection, Blimp1-YFP reporter SM (Fig. 4A–D) and polyclonal (Fig. 4E, 4F) CD4 T cells were analyzed based on PSGL1 and Ly6C. Our data are consistent with a previous study (47), where PSGL1^{hi}Ly6C^{hi} and PSGL1^{lo}Ly6C^{lo} exhibited strong expression of Blimp1$_{YFP}$ and Bcl6, respectively (Fig. 4C, 4D). However, we found that both Blimp1$_{YFP}^-$CXCR5$^+$(Bcl6$^+$) Tfh and Blimp1$_{YFP}^+$ CXCR5$^-$(Bcl6$^-$) Th1 cells were mixed in the PSGL1^{hi}Ly6C^{lo} gate (Fig. 4A, 4B, 4E, 4F).

Memory precursor CD8 T cells have been distinguished as early as 3.5 d in vivo after LCMV infection, on the basis of IL-2Rα expression (48), and differential IL-2 signaling can preferentially direct activated CD8 T cells to short-lived effector (perforin^{hi} Blimp1$^+$) or memory cell precursor (IL-7Rα$^+$Bcl6$^+$) fates (49). Given that differential IL-2Rα expression on early-memory precursor CD8 T cells versus terminal effector–biased CD8 T cells parallels differential IL-2Rα expression on early Tfh cells versus Th1 cells (Fig. 2) (9), we took an unbiased approach to ask whether Tfh differentiation pathway may share a molecular program with early-memory precursor CD8 T cells, identifiable as a transcriptional signature. Gene expression data for day 3.5 memory precursor and effector-biased CD8 T cells populations were compared with gene expression data for day 8 Tfh and Th1 CD4 T cell populations. The full data sets were queried for the set of all genes differentially expressed (≥2-fold) by Tfh cells compared with Th1 cells and also differentially expressed by early memory precursor CD8 T cells compared with short-lived effector–biased CD8 T cells. This screening was done irrespective of the directionality of the gene expression changes in each data set. A total of 173 gene transcripts satisfied these conditions (Supplemental Table I). Impressively, of the 173 gene expression changes, 95 genes were upregulated in both Tfh cells and memory precursor CD8 T cells, and 45 genes were downregulated in both Tfh cells and memory precursor CD8 T cells (Fig. 5A, Supplemental Table I). This gave a cumulative total of 140 of 173 gene expression changes being in a shared direction in Tfh cells and memory precursor CD8 T cells. Only a small number of genes did not exhibit shared directionality. This was a highly nonrandom distribution of shared directionality ($p = 1.0 \times 10^{-14}$), indicating the presence of a shared gene expression program between Tfh cells and memory precursor CD8 T cells. Bcl6 and Blimp1 both appear in this gene set in addition to many other genes with known or potential connections to memory cell development (Fig. 5B).

These "memory type" gene expression patterns were then tested for their ability to predict early gene expression differences in day 3 Tfh versus Th1 cells. RNA was isolated from sorted day 3 Tfh and Th1 cells (Fig. 2A) and analyzed for specific gene expression differences. Bcl6 and Blimp1 were confirmed to be strongly differentially expressed between early Tfh and Th1 cells (40-fold *Bcl6* mRNA difference, $p = 1 \times 10^{-6}$; 51-fold *Prdm1* difference, $p = 9.2 \times 10^{-5}$; Fig. 5C). In addition to *Bcl6*, the early fate-committed Tfh cells induced strong expression of genes that were also highly upregulated by memory precursors CD8 T cells (48), including *Tcf7* (38-fold; $p = 1 \times 10^{-6}$) (50), *Tox2* (14-fold; $p = 5 \times 10^{-6}$), and *Id3* (96-fold; $p = 2 \times 10^{-6}$) (51) (Fig. 5D). Interestingly, several cell surface receptors strongly associated with Tfh cell functions were unexpectedly predicted to be associated with memory programming (Fig. 5F) and indeed had strong expression differences between early Tfh and Th1 cells, including *Cd200* (11-fold; $p = 1.61 \times 10^{-6}$), *Btla* (5-fold; $p = 5.46 \times 10^{-6}$), and *Ly108* (3-fold; $p = 0.008$) (Fig. 5E). In contrast, genes that were strongly suppressed by memory precursor CD8 T cells, such as *Id2*, *Havcr2*, and *Il2ra*, were substantially downregulated by the early fate-committed Tfh cells compared with Th1 cell counterparts (Fig. 5G) (35, 48, 49, 52). Each predicted gene expression change tested was correct. This is consistent with the presence of an underlying gene expression profile linking part of Tfh cell biology with the generation of T cell memory.

Development of memory CD4 T cells

The findings regarding Tfh cell fate commitment and shared gene expression with memory precursor CD8 T cells led us to examine whether early differentiated Tfh cells may contribute to the CD4 T cell memory compartment after an acute viral infection. We transferred day 3 CD45.1$^+$ Tfh and Th1 SM cells into infection-matched CD45.2$^+$ recipients, which were then analyzed at immune memory time points (day 30–45 postinfection) (Fig. 6A). Strikingly, at memory time points, we found significantly more SM cells in early Tfh-recipient mice than in mice that received early Th1 cells ($p = 0.015$ at day 45; Fig. 6B) ($p = 0.0007$ at day

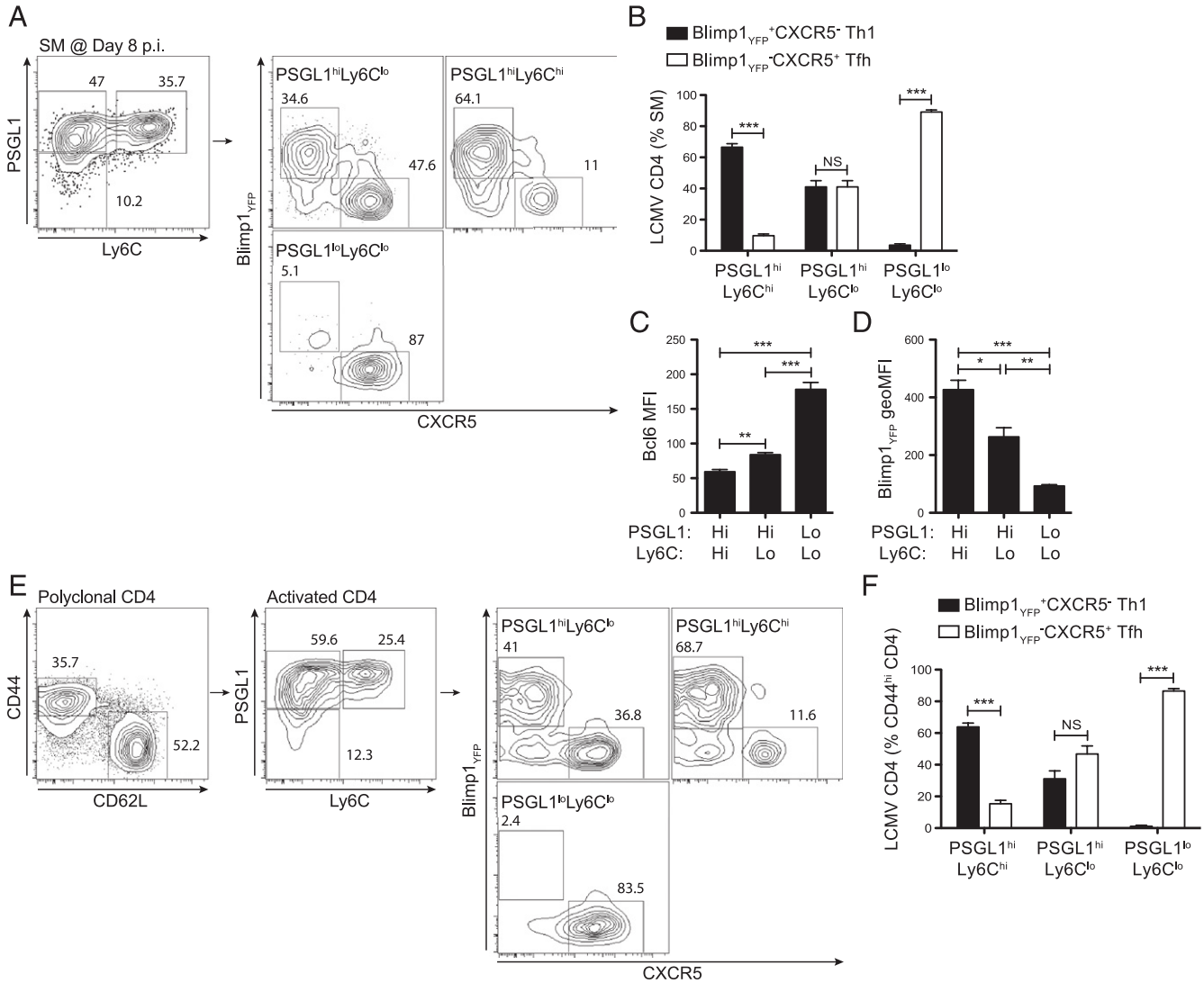

FIGURE 4. PSGL1^{hi}Ly6C^{lo} compartment consists of fully differentiated Tfh and Th1 cells. (**A**–**D**) LCMV-specific Blimp1-YFP SM (CD45.1$^+$) CD4 T cells were divided into three compartments (PSGL1^{hi}Ly6C^{hi}, PSGL1^{hi}Ly6C^{lo}, and PSGL1^{lo}Ly6C^{lo}) in B6 (CD45.2$^+$) mice at day 8 postinfection. The three populations were further separated into Blimp1$_{YFP}^+$CXCR5$^-$ Th1 and Blimp1$_{YFP}^-$CXCR5$^+$ Tfh cells. (A) Representative FACS plots of SM cells. Gates indicate PSGL1^{hi}Ly6C^{hi}, PSGL1^{hi}Ly6C^{lo}, and PSGL1^{lo}Ly6C^{lo} SM populations (*left panel*). Blimp1$_{YFP}$ and CXCR5 expression was analyzed (*right panel*). (B) Percentages of Blimp1$_{YFP}^+$CXCR5$^-$ non-Tfh and Blmp1$_{YFP}^-$CXCR5$^+$ Tfh cells from PSGL1^{hi}Ly6C^{hi}, PSGL1^{hi}Ly6C^{lo}, and PSGL1^{lo}Ly6C^{lo} gates calculated. Bcl6 mean fluorescence intensities (C) and Blimp1$_{YFP}$ geometric mean fluorescence intensities (D) calculated. (**E** and **F**) Blimp1-YFP B6 mice were infected with LCMV and activated (CD44^{hi}CD62L$^-$) CD4 T cells were analyzed for PSGL1 and Ly6C expression. (E) Blimp1$_{YFP}$ and CXCR5 expression was further examined. (F) Relative frequencies of Blimp1$_{YFP}^+$CXCR5$^-$ Th1 and Blimp1$_{YFP}^-$CXCR5$^+$ Tfh cells. n = 3–4 mice/group. *$p <$ 0.05, **$p < 0.01$, ***$p < 0.001$, shown as mean and SEM.

30; data not shown). Furthermore, the vast majority of transferred Tfh cells were found as CXCR5$^+$ Tfh cells (85 ± 2 and 78 ± 5% of total transferred cells at day 30 and 45 p.i., respectively; Fig. 6B). In sharp contrast, early Th1 cells failed to maintain their phenotype and were identified as three populations: Blimp1$_{YFP}^+$CXCR5$^-$, Blimp1$_{YFP}^-$CXCR5$^-$, and Blimp1$_{YFP}^-$CXCR5$^+$ (Fig. 6B). Early Tfh cell–recipient mice had a small but significant increase in Bcl6 expression compared with Th1 cell recipient mice (Fig. 6C). Taken together, our data demonstrate that large numbers of memory CD4 T cells are derived from the early Tfh cell population, and long-term survival of these cells is associated with Bcl6 expression.

Long-term survival of Tfh cells is associated with re-expression of IL-7Rα during the late, but not early, Tfh differentiation program

Our data implied that Tfh cells acquired a cell-intrinsic survival program during differentiation and thus could remain at higher frequencies at memory points (Fig. 6). IL-7 signaling through IL-7Rα is critical for long-term survival of memory CD4 T cells. A lack of either IL-7 or IL-7Rα expression leads to defective development and maintenance of memory CD4 T cells (53, 54). Surface IL-7Rα expression is also associated with long-term survival of memory CD8 T cells (46). Therefore, we investigated the expression levels of IL-7Rα on memory Tfh cells (CXCR5$^+$Blimp1$_{YFP}^-$) and Th1 cells (CXCR5$^-$Blimp1$_{YFP}^+$) in respective recipient mice. Both Tfh and Th1 memory cells expressed higher levels of IL-7Rα than naive CD4 T cells (CD44^{lo}) (Fig. 7A). Interestingly, IL-7Rα was statistically higher on memory Tfh cells than Th1 cells ($p = 0.02$; Fig. 7A). We then examined whether differences in IL-7Rα expression in Tfh cells occur early during the immune responses. At 3 d after LCMV infection, IL-7Rα was strongly downregulated by both Tfh and Th1 cells (Fig. 7B). Strikingly, at day 8, the peak of the CD4 response to LCMV infection, we found that IL-7Rα was selectively re-expressed by a fraction of

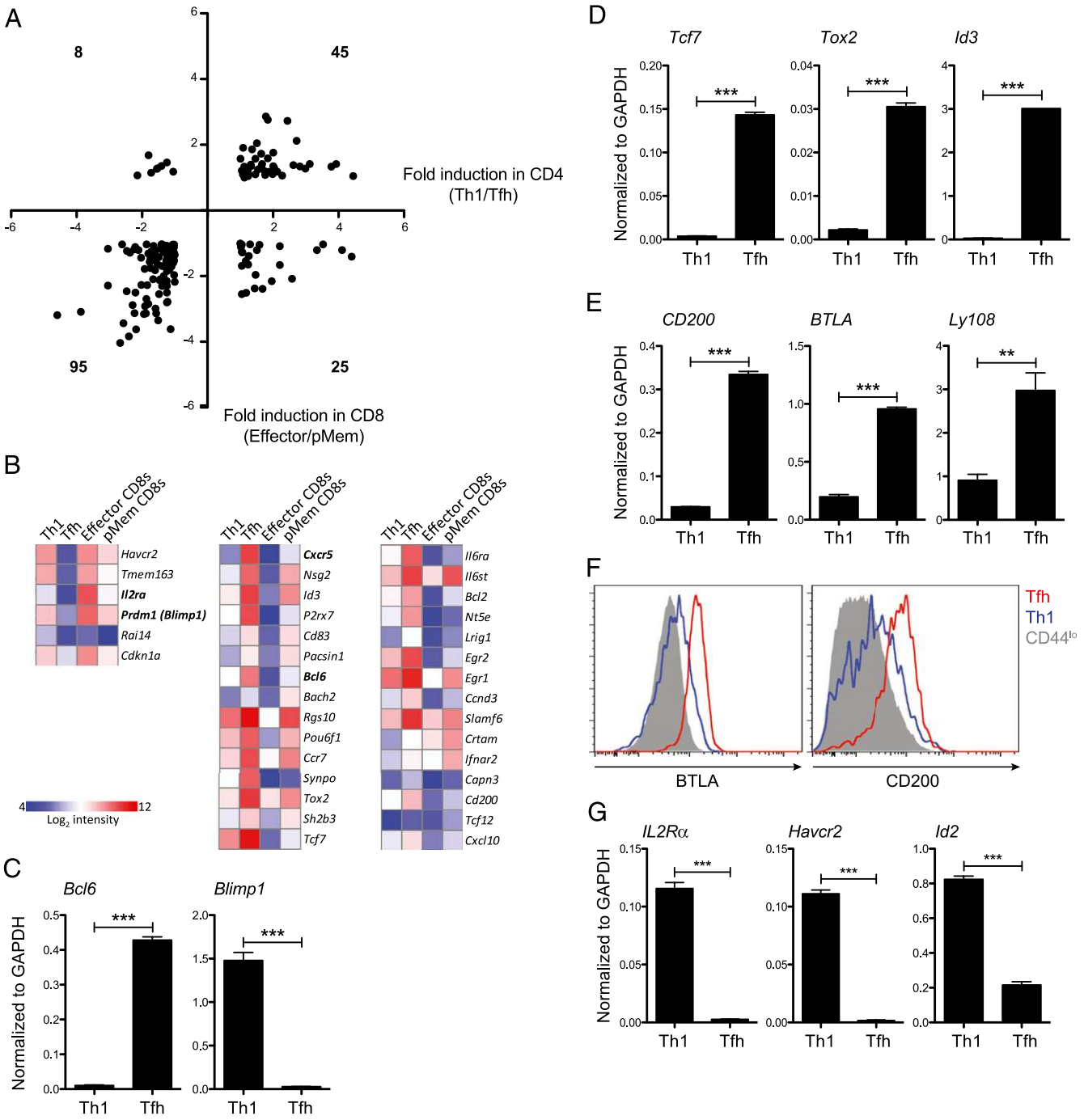

FIGURE 5. Early fate-committed Tfh cells share a molecular signature with memory precursor CD8 T cells. Microarray data, obtained from three independent studies were normalized and analyzed (described in detail in *Materials and Methods*). (**A**) A total of 173 genes that were identified to be used commonly by both CD4 and CD8 T cells are shown in a scatter plot. Bold numbers mean number of genes in each quadrant. (**B**) Heat map of mRNA expression of 36 representative genes. (**C**–**E** and **G**) Tfh (IL-2Rα$^-$Blimp1$_{YFP}^-$) and Th1 (IL-2Rα$^+$Blimp1$_{YFP}^+$) cells were sorted 72 h after LMCV infection (Fig. 2A). Quantitative PCR analysis was performed with isolated mRNA for analysis of relative expressions of *Bcl6* and *Blimp1* (C), *Tcf7*, *Tox2*, and *Id3* (D), *CD200*, *BTLA*, and *Ly108* (*Slamf6*) (E), and *Il2ra*, *Havcr2*, and *Id2* (G). Normalized to *Gapdh*. (**F**) Surface expressions of BTLA and CD200 by Tfh (red) and Th1 (blue) cells compared with those of naive CD4 (gray filled) cells. Data are representative of two independent experiments with three replicates each (C–E, G). $^{**}p < 0.01$, $^{***}p < 0.001$, shown as mean and SEM.

CXCR5$^+$ CD4 T cells (20 ± 2% IL7Rα$^+$ Tfh; $p = 4.4 \times 10^{-5}$ for Tfh versus Th1) (Fig. 7C, 7D). IL-7Rα re-expression on Tfh cells became even more dramatic 11 d postinfection. More than 75% of Tfh cells regained IL-7Rα expression ($p = 2.8 \times 10^{-6}$ for Tfh versus Th1) (Fig. 7E, 7F). Taken together, our data demonstrate that Tfh cells exhibit superior re-expression of IL-7Rα to Th1 cells during the late stages of an LCMV infection, and it is associated with a survival advantage of Tfh cells at memory time points of the immune response to LCMV infection (Fig. 6A).

Proliferation responsiveness of mature Tfh cells

Abundance of memory cells after early Tfh cell transfers compared with early Th1 cell transfers as well as selective re-expression of

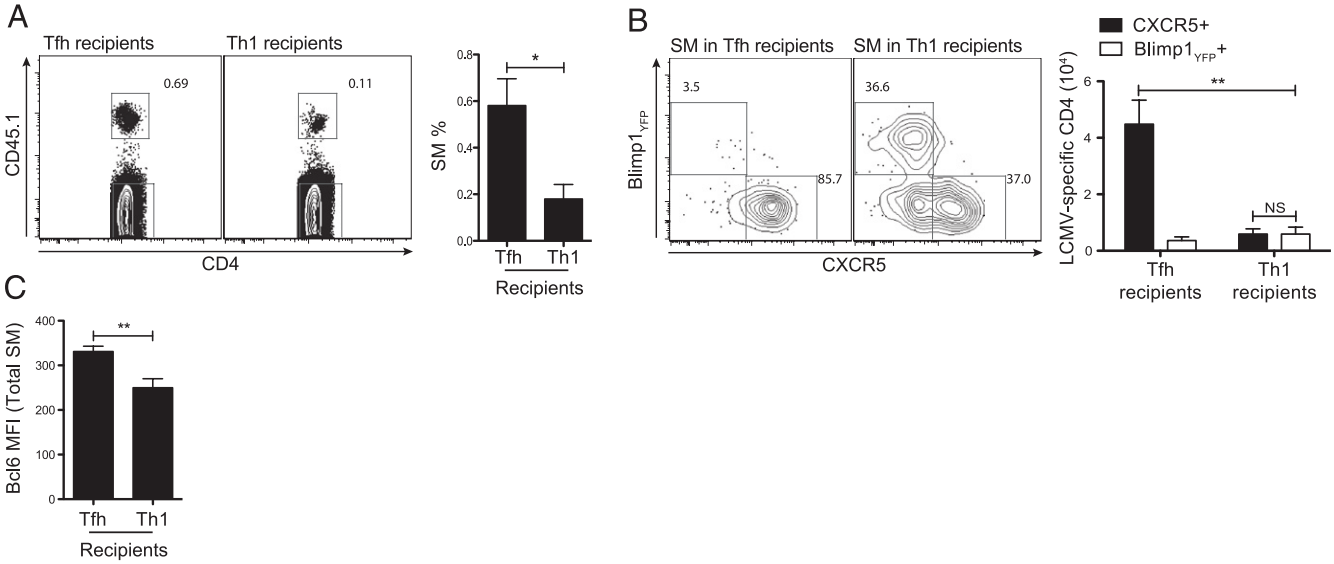

FIGURE 6. Fate determined Tfh cells contribute to CD4 T cell memory. (**A**) Day 3 Tfh (IL-2Rα$^-$Blimp1$_{YFP}^-$) and Th1 (IL-2Rα$^+$Blimp1$_{YFP}^+$) cells were sorted and transferred into separate groups of infection-matched B6 mice (Fig. 2A). Tfh and Th1 recipients were analyzed 45 d after LCMV infection. Representative FACS plots for SM cells in the spleens of Tfh and Th1 cell recipients. Quantifications determined as percentages of the number of SM cells in total CD4 T cells. (**B**) Th1 (Blimp1$_{YFP}^+$CXCR5$^-$) and Tfh (Blimp1$_{YFP}^-$CXCR5$^+$) cells gated on total SM cells of respective recipient mice. Quantitation made as the numbers of Th1 (white) and Tfh (black) cells in spleen. (**C**) Bcl6 mean fluorescence intensities of total donor cells in 45-d LCMV-infected recipient mice. Data are representative of two experiments at two different memory time points (days 30 and 45) after LCMV infection. $n = 5–6$ mice/group. $^*p < 0.05$, $^{**}p < 0.01$, shown as mean and SEM.

IL-7Rα of mature Tfh cells led us to examine the proliferation capacity of fully differentiated Tfh cells in greater detail. To address this point, we sorted Tfh cells (PD-1^{hi}CXCR5$^+$Blimp1$_{YFP}^-$) and Th1 cells (PD-1^{int}CXCR5$^-$Blimp1$_{YFP}^+$) at day 8 after LCMV infection, the peak of the CD4 T cell response (Fig. 8A, 8B). The cells were then labeled with a proliferation tracking dye and cultured in the presence or absence of anti-CD3/28 mAbs. In the absence of antigenic stimulation signals, neither day 8 Th1 or Tfh

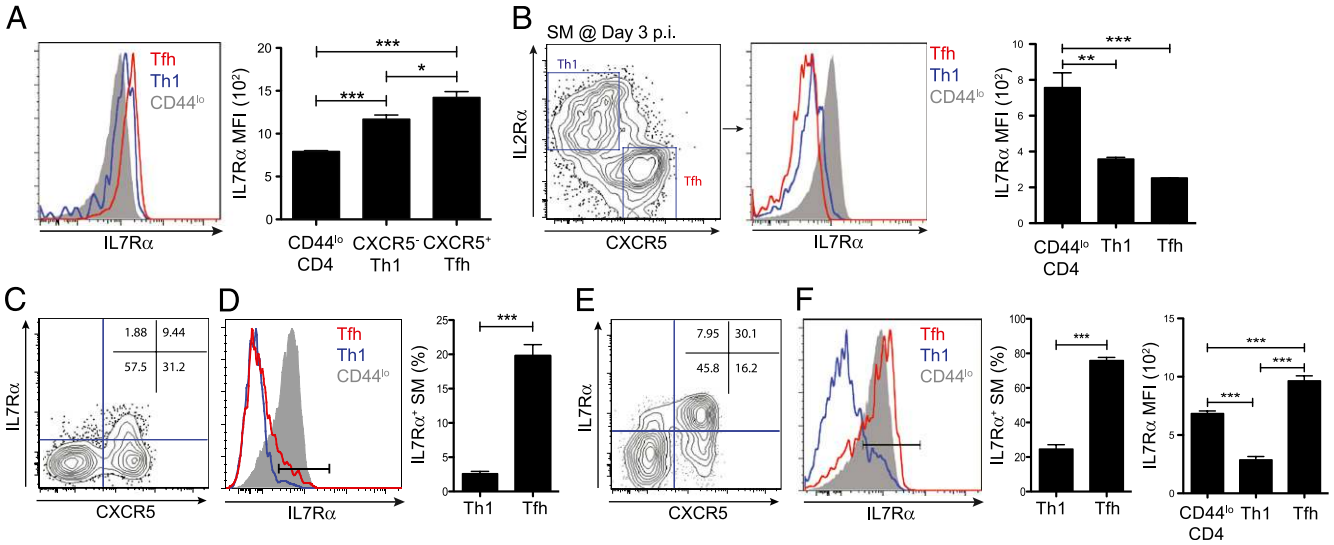

FIGURE 7. Tfh cells regain IL-7Rα expressions at the peak of the immune response and maintain higher expression of IL-7Rα in memory phase. (**A**) Overlaid histograms for IL-7Rα expression by CD44^{lo} CD4 T cells in a naive mouse (gray filled) and Th1 (blue) and Tfh (red) cells in Th1- and Tfh-recipient mice, respectively, from day 45 after LCMV-infected B6 mice. Quantitation calculated as mean fluorescence intensities. Data are representative of two experiments that were singly done at two different memory time points (days 30 and 45) after LCMV infection. (**B**) Naive SM (CD45.1$^+$) CD4 T cells were transferred into B6 mice that were subsequently infected with LCMV. Th1 (IL-2Rα$^+$CXCR5$^-$) and Tfh (IL-2Rα$^-$CXCR5$^+$) cells were obtained from 3-d LCMV-infected spleens. IL-7Rα expression depicted by overlaid histograms (CD44^{lo} CD4 T cells in a naive mouse, shown in gray filled; Th1 (blue) and Tfh (red) of 3-d LCMV-infected mice). (**C–F**) Naive SM (CD45.1$^+$) CD4 T cells were transferred into B6 mice that were subsequently infected with LCMV. SM cells were analyzed at day 8 (C, D) and day 11 (E, F) after LCMV infection. (C) Representative FACS plots of SM cells 8 d after LCMV infection. (D) Overlaid histograms for IL-7Rα expression by CD44^{lo} CD4 T cells in a naive mouse (gray filled) and Th1 (blue) and Tfh (red) cells from LCMV-infected mice at day 8. The bar indicates IL-7Rα^{hi}–expressing cells. Quantitation done as IL-7Rα^{hi} percentage of Th1 (CXCR5$^-$) and Tfh (CXCR5$^+$) cells. (E) SM cells were gated by CD45.1 expression and were subsequently analyzed by IL-7Rα and CXCR5 expression. Numbers in each quadrant indicate frequencies of populations among total SM cells. (F) Overlaid histograms for IL-7Rα expression by CD44^{lo} naive CD4 (gray filled) of naive mouse and Th1 (blue) and Tfh (red) cells from 11-d LCMV-infected spleens (*left panel*). The bar indicates IL-7Rα–expressing cells. Quantifications made as percentages of IL-7Rα expressing cells within Th1 versus Tfh cells (*middle panel*) and total IL-7Rα mean fluorescence intensities (*right panel*). Data are representative of two independent experiments (B–F). $n = 4–6$ mice/group. $^*p < 0.05$, $^{**}p < 0.01$, $^{***}p < 0.001$, shown as mean and SEM.

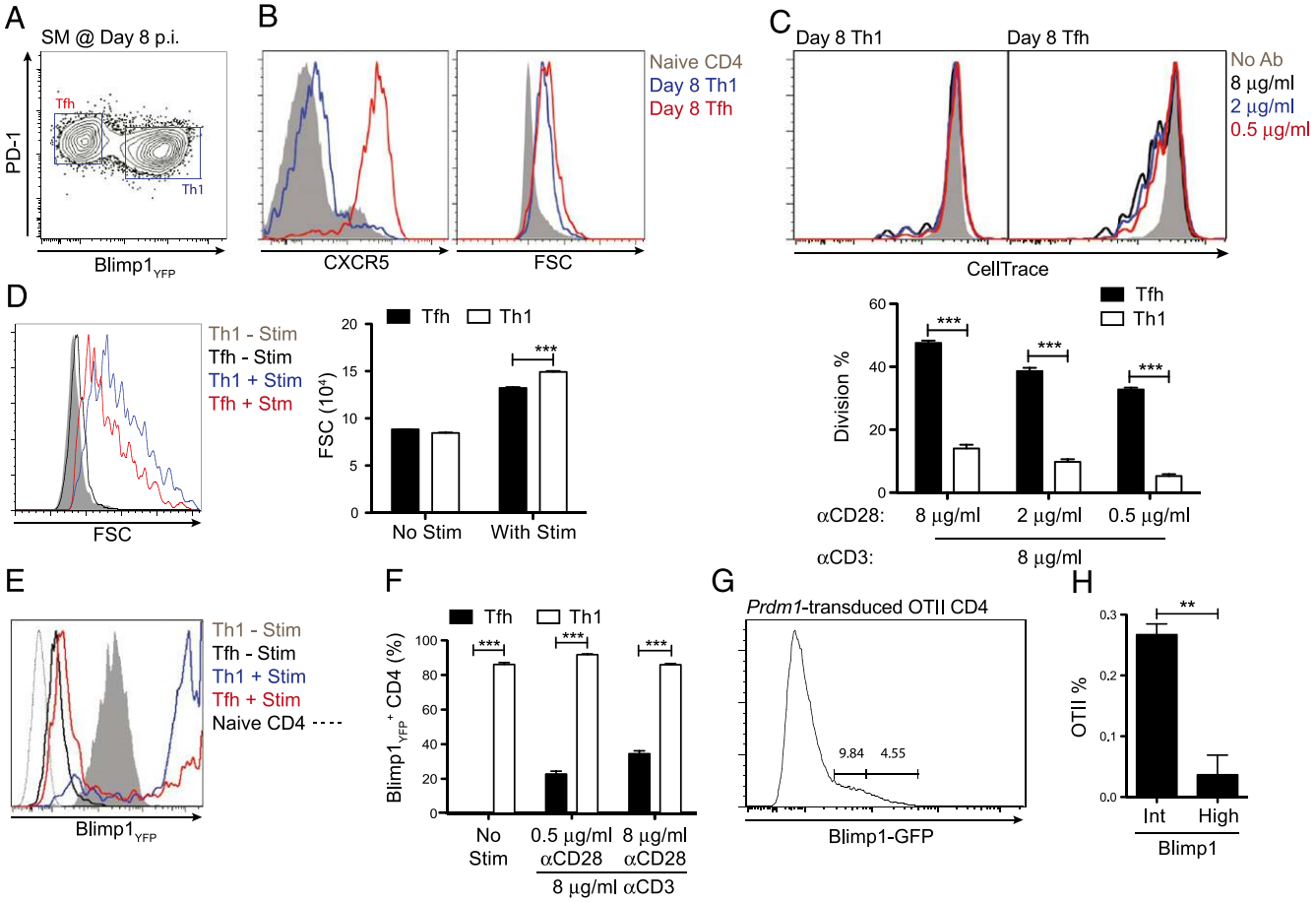

FIGURE 8. Tfh cells respond to antigenic restimulation signals. (**A**) Schematic diagram of Tfh (PD-1^{hi}Blimp1$_{YFP}^{-}$) and Th1 (PD-1^{int}Blimp1$_{YFP}^{+}$) SM cells sorted from day 8 LCMV-infected mice. (**B**) Representative overlaid histograms for CXCR5 expression and cell size of Th1 (blue) and Tfh (red) cells. (**C**) Overlaid histograms show proliferations of Th1 (*left panel*) and Tfh (*right panel*) cells in the absence of stimulation (gray filled) or in the presence of 8 μg/ml anti-CD3 mAbs with different amount of anti-CD28 mAbs (8 μg/ml in black, 2 μg/ml in blue, and 0.5 μg/ml in red) (*upper panels*). Quantifications made as percentages of divided cells by Tfh (black) and Th1 (gray) cells 3 d after in vitro culture (*lower panel*). (**D**) Cell sizes determined by forward light scatter of activated Tfh (red) and Th1 (blue) cells compared with those of nonactivated Tfh (black) and Th1 (gray filled) cells. Quantitation made as mean fluorescence intensities of forward light scatter (FSC). (**E**) Level of Blimp1$_{YFP}$ expression depicted by overlaid histograms of activated Tfh (red) and Th1 (blue) cells compared with those of nonactivated Tfh (black) and Th1 (gray filled) cells. Dashed lines show background level of Blimp1$_{YFP}$ by CD44^{lo} naive CD4 T cells in naive mouse. (**F**) Quantitation made as percentages of Blimp1$_{YFP}$-expressing cells in indicated culture conditions. Data are representative of two or more independent experiments using three to five replicate wells per group. (**G** and **H**) OTII CD4 (CD45.1^{+}) T cells were transduced with a retroviral vector that expresses Blimp1 with GFP. (G) Blimp1^{int} (GFP^{int})- and Blimp1^{hi} (GFP^{hi})-expressing cells were sorted based on GFP expression and transferred into B6 (CD45.2^{+}) mice. (H) Expansion of OTII CD4 T cells were measured 8 d after NP-OVA immunization as percentage of total CD4 T cells. n = 3–4/group. $^{**}p < 0.01$, $^{***}p < 0.001$, shown as mean and SEM.

cells proliferated in vitro (Fig. 8C, gray-filled histograms). However, once TCR and costimulation signals were provided, Tfh cells proliferated well (Fig. 8C, colored lines), whereas Th1 cells proliferated poorly (bar graph: $p = 4.0 \times 10^{-6}$, 4.3×10^{-6}, and 4.8×10^{-7} for 8, 2, and 0.5 μg/ml anti-CD28, respectively; Fig. 8C). This was quite different from the early Th1 cells, which proliferated vigorously even in the absence of TCR signals (Fig. 3D). Interestingly, although Tfh cells required TCR stimulation for proliferation at day 8, we found that costimulatory signaling via CD28 was minimally involved (48 ± 1 and 33 ± 0.8% proliferations by 8 and 0.5 μg/ml anti-CD28, respectively; Fig. 8C). We speculated that early TCR signaling may be altered in fully differentiated Th1 effector cells such that glycolytic metabolism was limited, preventing proliferation. We therefore examined Th1 cell blasting following TCR stimulation. Th1 cells robustly increased cell size in response to TCR signals ($p = 7.5 \times 10^{-5}$; Fig. 8D), indicating that the block in Th1 proliferation was far downstream of TCR signaling and glycolytic metabolism. We therefore investigated whether different proliferation capacities of Tfh and Th1 cells were associated with Blimp1 expression, a highly antiproliferative molecule (55). Th1 cells expressed Blimp1$_{YFP}$ at 15-fold higher levels than Tfh cells ($p = 5.3 \times 10^{-8}$, no stimulation; Fig. 8E). After 72 h of restimulation, although only a small fraction of Tfh cells could express Blimp1$_{YFP}$, Th1 cells further increased Blimp1$_{YFP}$ expression (Fig. 8E, 8F). Moreover, in vivo experiments demonstrated that high expression of Blimp1 blocks CD4 T cell proliferation. OVA-specific TCRtg (OTII) CD4 T cells transduced with a Blimp1 expressing retroviral expression vector (Blimp1-GFP) exhibited significantly less proliferation in vivo at day 8 after NP-Ova immunization when the OTII CD4 T cells expressed high levels of Blimp1 versus intermediate levels of Blimp1 (Blimp1^{int} versus Blimp1^{hi}, $p = 0.002$; Fig. 8G, 8H). In summary, the capacity of mature Tfh cells to respond to TCR-mediated activation signals at the peak of the immune response was associated with more Tfh cells being found at memory time points after LCMV infection (Fig. 6A), possibly because of proliferation induced by Ag presentation by germinal center B cells and the lack of Blimp1 expression by Tfh cells. Taken together,

these data show that Bcl6$^+$CXCR5$^+$ Tfh cells become fate committed early after an acute viral infection and acquire distinct proliferation and survival capacities compared with Th1 cells.

Discussion

The stability of Tfh cells and the stability of Bcl6 expression in Tfh cells have been questions of great interest (56), accentuated by recent findings of plasticity of many types of differentiated CD4 T cells (12, 21, 57). Recent work has revealed plasticity of Tfh cells (12–14, 58). Conversion of transferred Tfh cells into Th1 cells was observed during a recall response to influenza virus infection in recipient mice (58). However, similar conversions have been reported by both in vitro– and in vivo–activated Th1, Th2, induced regulatory T cells, and Th17 cells for reprogramming to other Th differentiation program (23, 59, 60). There are numerous examples that, if the external forces are strong enough, then differentiated CD4 T cells can change their differentiation programming to respond to new environmental cues, even including extreme events such as Th2 cells acquiring Th1 differentiation in vivo (61). As such, it is unclear whether Tfh cells possess any more plasticity than other CD4 T cell differentiation programs. Therefore, we focused on cell fate commitment within physiological environment. As described in this study, we found that early differentiated Tfh (or Th1) cells maintained their original differentiation pathway in recipient mice during the course of LCMV infection and hence were cell fate committed. Our data are consistent with a recent study, which demonstrates transferred Tfh and Th2 cells remained stable in recipient mice upon Ag challenge (19). Therefore, our data support the concept that Tfh cells primarily develop as an independent differentiation pathway, starting from the earliest stages of DC priming (9, 40). However, this does not rule out the possibility that there are multiple pathways to Tfh cell differentiation and that differentiated cells may convert to Tfh cells under strong environmental cues (20, 62).

Similar to stem cells (63) and a variety of cell types studied in the context of developmental biology where non-cell autonomous positional cues and microanatomical niches are a central attribute of cell fate determination, maintenance of Tfh cell fate commitment differentiation is dependent on external factors. Tfh cells are lost if forced into a nonphysiological environment (Fig. 3). The extrinsic signals provided by B cells include Ag presentation, ICOS ligand, and possibly other Tfh cell maintenance factors. These signals are critical for Tfh cells to maintain a high Bcl6 to T-bet ratio. Lack of those external signals in μMT mice (2, 6, 9, 44) or in mice where ICOS–ICOS ligand interaction is specifically blocked during cognate B:T interaction (9, 40) leads to reduced expression of Bcl6. Bcl6 can repress T-bet (7). Proinflammatory cytokines in LCMV-infected animals may continuously drive T-bet expression. Hence, a concomitant inverted Bcl6 to T-bet ratio (Bcl6 $<$ T-bet) is observed in Tfh cells of μMT mice (data not shown), which putatively leads to the DNA-binding domain of Bcl6 being masked by T-bet (64), causing a loss of Bcl6-mediated Blimp1 repression. As a result, CXCR5$^+$ Tfh cells in Tfh-recipient μMT mice expressed Blimp1 at a much higher level compared with Tfh cells in B6 mice (Fig. 2).

The rigid requirement of Ag presentation, initially by DCs and followed by B cells, is one of the unique features for Tfh differentiation (2, 6, 9, 40, 42, 43). Relatively short TCR stimulation is sufficient for CD8 T cells to proliferate and differentiate into effector cells (65, 66). In sharp contrast, CD4 T cells are highly dependent on Ag recognition to continue proliferation and complete their differentiation (67). Our in vitro experiments with ex vivo Tfh versus Th1 cells from day 3 LCMV–infected animals clearly show that Tfh cells require Ag presentation for each round of cell division. Notably, Tfh cells obtained at the peak response to LCMV infection proliferated upon TCR stimulation whereas Th1 cells did not; therefore, Tfh differentiation program could be biased toward development of memory CD4 T cells that maintain TCR-mediated proliferative capacity. Along with previous work that demonstrated generation of memory CD4 T cells by CXCR5$^+$ CD4 T cells (18, 19, 33, 58), the current study indicates early Tfh differentiation pathway shares properties with memory CD4 T cells. However, we do not agree with the conclusion that the CXCR5$^+$ cells were not Tfh cells (18). That conclusion was based on a lack of short-term colocalization with B cells, but that cell transfer was restricted to only a subfraction of the CXCR5$^+$PD1^{lo} population that were also highly expressing CCR7 (18). Contrary to that conclusion, the CXCR5$^+$PD1^{lo} cells were dependent on B cells for their development, indicating the CXCR5 expression was functional for colocalizing with B cells (18). The majority of day 8 CXCR5$^+$ CD4 T cells localize to B cell follicle and T/B border in independent studies (33, 68). Our data demonstrate that the vast majority of all CXCR5$^+$ CD4 T cells in a viral infection develop from a Bcl6$^+$CXCR5$^+$ early Tfh cell population.

Bcl6 has been previously implicated in memory T cell development, particularly memory CD8 T cell development (32, 35, 54). By cell transfer experiments, we showed that Ag-experienced CD4 T cells rapidly acquired preferential cell fates associated with differential Bcl6 and Blimp1 expression. Our data in this study indicate that some functions of the Bcl6–Blimp1 regulatory axis are shared in CD4 T cells and CD8 T cells and control a gene expression program regulating memory formation. Preferential re-expression of IL-7Rα by Bcl6-expressing Tfh cells (Fig. 7) was a striking indication that this relationship was deeper than it first appeared. Our data also show that Tfh cells retained an enhanced capacity to respond to TCR stimulation compared with Th1 cells. This parallels observations for memory precursor CD8 T cells (35). These relationships between Tfh cell biology and memory T cell biology appear to repeatedly center on the Bcl6–Blimp1 signaling axis. Notably, Tfh cells were lost in the absence of B cells, in agreement with previous observations of B cell–dependent memory CD4 T cell development (69), providing another connection between Bcl6, Tfh cells, and CD4 T cell memory. Meta-analysis of Tfh cell and memory precursor CD8 T cell gene expression revealed potential genes that may form a transcriptional regulatory network with Bcl6 to facilitate memory T cell formation (Fig. 5). *Tcf-7*, which encodes Tcf-1, is a downstream effector of the wnt signaling pathway and was shown to be required for CD8 T cell central memory development (50, 70). However, data of Prlic and Bevan argues against the requirement of wnt signaling in memory T cell formation because they observed a normal memory formation in T cell specific β-catenin–deficient mice (71). Further investigation is required to address whether memory formation of T cells could be regulated by β-catenin–independent activation of Tcf-1. Id proteins partner with E proteins to modulate a wide range of lymphocyte differentiation processes (72), and Id proteins appear to have partially overlapping and partially distinct functions. *Id2*-deficient CD8 T cells failed to differentiate into effector CD8 T cells, whereas *Id2*-deficient memory precursor CD8 T cell development was relatively intact (52, 73–75). Recent data suggest that Id proteins have important but complex roles in CD4 T cell fates (51). Collectively, our data indicate that CD4 and CD8 T cells share a common molecular signature involving Bcl6 for development of memory precursor cells.

Given these findings, it is of interest to understand how Bcl6 facilitates memory T cell formation. Our data indicate IL-7Rα is somehow involved, and IL-7Rα has an important role in long-term

survival of memory CD4 T cells (46, 53, 76). Selective IL-7Rα expression identifies memory precursor CD8 T cells (46). Even though IL-7Rα expression alone is not sufficient for identifying memory precursor of CD4 T cells (47), in this study, we show that IL-7Rα expression was preferentially regained by Tfh cells. All available data indicate that Bcl6 is an obligatory transcriptional repressor (77, 78), suggesting that preferential upregulation of IL-7Rα is not due to direct activity of Bcl6 at the *Il7Ra* gene, but it could be due to Bcl6-mediated repression of an intermediary transcriptional repressor, such as Blimp-1 (35). In addition, these different CD4 T cell fates were associated with differential IL-2Rα expression early. A similar process is seen with early differentiating CD8 T cells (48, 49). It is striking that IL-2R and IL-7R repeatedly appear in opposition when comparing T cell populations, with IL-2R favoring terminal effector T cell differentiation and IL-7R expression favoring memory T cell development.

Vaccines are predicated on the existence of immunological memory. Memory T cells develop from a fraction of the activated T cells that survive long term and can undergo recall responses to the same Ag (79–81). Recent human studies support the conclusion that $CXCR5^+CD45RO^+$ CD4 T cells are functional memory Tfh cells (82). Human genetic data also supports this conclusion, because rare individuals with *Icos* gene deletions specifically lack $CXCR5^+CD45RO^+$ CD4 T cells (83), and ICOS is required for Tfh cell differentiation (9, 40). In this study, we found that day 3 $Bcl6^+CXCR5^+$ Tfh cells are precursors of memory Tfh cells. Given that memory T cells are important for many developing vaccine strategies, and Tfh cell function is likely essential for virtually all humoral immunity based vaccine strategies, regulation of Bcl6 in T cells has promise for providing key insights into understanding molecular regulation of both Tfh cell development and memory T cell formation.

Acknowledgments

We thank Dr. Danelle Eto and Robin Kageyama for technical support for this work.

Disclosures

The authors have no financial conflicts of interest.

References

1. Crotty, S. 2011. Follicular helper CD4 T cells (TFH). *Annu. Rev. Immunol.* 29: 621–663.
2. Haynes, N. M., C. D. C. Allen, R. Lesley, K. M. Ansel, N. Killeen, and J. G. Cyster. 2007. Role of CXCR5 and CCR7 in follicular Th cell positioning and appearance of a programmed cell death gene-1high germinal center-associated subpopulation. *J. Immunol.* 179: 5099–5108.
3. Zotos, D., J. M. Coquet, Y. Zhang, A. Light, K. D'Costa, A. Kallies, L. M. Corcoran, D. I. Godfrey, K.-M. Toellner, M. J. Smyth, et al. 2010. IL-21 regulates germinal center B cell differentiation and proliferation through a B cell-intrinsic mechanism. *J. Exp. Med.* 207: 365–378.
4. O'Shea, J. J., and W. E. Paul. 2010. Mechanisms underlying lineage commitment and plasticity of helper $CD4^+$ T cells. *Science* 327: 1098–1102.
5. Yu, D., S. Rao, L. M. Tsai, S. K. Lee, Y. He, E. L. Sutcliffe, M. Srivastava, M. Linterman, L. Zheng, N. Simpson, et al. 2009. The transcriptional repressor Bcl-6 directs T follicular helper cell lineage commitment. *Immunity* 31: 457–468.
6. Johnston, R. J., A. C. Poholek, D. DiToro, I. Yusuf, D. Eto, B. Barnett, A. L. Dent, J. Craft, and S. Crotty. 2009. Bcl6 and Blimp-1 are reciprocal and antagonistic regulators of T follicular helper cell differentiation. *Science* 325: 1006–1010.
7. Nurieva, R. I., Y. Chung, G. J. Martinez, X. O. Yang, S. Tanaka, T. D. Matskevitch, Y.-H. Wang, and C. Dong. 2009. Bcl6 mediates the development of T follicular helper cells. *Science* 325: 1001–1005.
8. Kroenke, M. A., D. Eto, M. Locci, M. Cho, T. Davidson, E. K. Haddad, and S. Crotty. 2012. Bcl6 and Maf cooperate to instruct human follicular helper CD4 T cell differentiation. *J. Immunol.* 188: 3734–3744.
9. Choi, Y. S., R. Kageyama, D. Eto, T. C. Escobar, R. J. Johnston, L. Monticelli, C. Lao, and S. Crotty. 2011. ICOS receptor instructs T follicular helper cell versus effector cell differentiation via induction of the transcriptional repressor Bcl6. *Immunity* 34: 932–946.
10. Kerfoot, S. M., G. Yaari, J. R. Patel, K. L. Johnson, D. G. Gonzalez, S. H. Kleinstein, and A. M. Haberman. 2011. Germinal center B cell and T follicular helper cell development initiates in the interfollicular zone. *Immunity* 34: 947–960.
11. Kitano, M., S. Moriyama, Y. Ando, M. Hikida, Y. Mori, T. Kurosaki, and T. Okada. 2011. Bcl6 protein expression shapes pre-germinal center B cell dynamics and follicular helper T cell heterogeneity. *Immunity* 34: 961–972.
12. Lu, K. T., Y. Kanno, J. L. Cannons, R. Handon, P. Bible, A. G. Elkahloun, S. M. Anderson, L. Wei, H. Sun, J. J. O'Shea, and P. L. Schwartzberg. 2011. Functional and epigenetic studies reveal multistep differentiation and plasticity of in vitro-generated and in vivo-derived follicular T helper cells. *Immunity* 35: 622–632.
13. Nakayamada, S., Y. Kanno, H. Takahashi, D. Jankovic, K. T. Lu, T. A. Johnson, H. W. Sun, G. Vahedi, O. Hakim, R. Handon, et al. 2011. Early Th1 cell differentiation is marked by a Tfh cell-like transition. *Immunity* 35: 919–931.
14. Oestreich, K. J., S. E. Mohn, and A. S. Weinmann. 2012. Molecular mechanisms that control the expression and activity of Bcl-6 in TH1 cells to regulate flexibility with a TFH-like gene profile. *Nat. Immunol.* 13: 405–411.
15. Johnston, R. J., Y. S. Choi, J. A. Diamond, J. A. Yang, and S. Crotty. 2012. STAT5 is a potent negative regulator of TFH cell differentiation. *J. Exp. Med.* 209: 243–250.
16. Ballesteros-Tato, A., B. León, B. A. Graf, A. Moquin, P. S. Adams, F. E. Lund, and T. D. Randall. 2012. Interleukin-2 inhibits germinal center formation by limiting T follicular helper cell differentiation. *Immunity* 36: 847–856.
17. Vinuesa, C. G., and J. G. Cyster. 2011. How T cells earn the follicular rite of passage. *Immunity* 35: 671–680.
18. Pepper, M., A. J. Pagán, B. Z. Igyártó, J. J. Taylor, and M. K. Jenkins. 2011. Opposing signals from the Bcl6 transcription factor and the interleukin-2 receptor generate T helper 1 central and effector memory cells. *Immunity* 35: 583–595.
19. Liu, X., X. Yan, B. Zhong, R. I. Nurieva, A. Wang, X. Wang, N. Martin-Orozco, Y. Wang, S. H. Chang, E. Esplugues, et al. 2012. Bcl6 expression specifies the T follicular helper cell program in vivo. *J. Exp. Med.* 209: 1841–1852, S1–S24.
20. Zaretsky, A. G., J. J. Taylor, I. L. King, F. A. Marshall, M. Mohrs, and E. J. Pearce. 2009. T follicular helper cells differentiate from Th2 cells in response to helminth antigens. *J. Exp. Med.* 206: 991–999.
21. Bluestone, J. A., C. R. Mackay, J. J. O'Shea, and B. Stockinger. 2009. The functional plasticity of T cell subsets. *Nat. Rev. Immunol.* 9: 811–816.
22. Murai, M., O. Turovskaya, G. Kim, R. Madan, C. L. Karp, H. Cheroutre, and M. Kronenberg. 2009. Interleukin 10 acts on regulatory T cells to maintain expression of the transcription factor Foxp3 and suppressive function in mice with colitis. *Nat. Immunol.* 10: 1178–1184.
23. Zhou, L., M. M. W. Chong, and D. R. Littman. 2009. Plasticity of $CD4^+$ T cell lineage differentiation. *Immunity* 30: 646–655.
24. Lee, S. K., D. G. Silva, J. L. Martin, A. Pratama, X. Hu, P.-P. Chang, G. Walters, and C. G. Vinuesa. 2012. Interferon-γ excess leads to pathogenic accumulation of follicular helper T cells and germinal centers. *Immunity* 37: 880–892.
25. Cretney, E., A. Xin, W. Shi, M. Minnich, F. Masson, M. Miasari, G. T. Belz, G. K. Smyth, M. Busslinger, S. L. Nutt, and A. Kallies. 2011. The transcription factors Blimp-1 and IRF4 jointly control the differentiation and function of effector regulatory T cells. *Nat. Immunol.* 12: 304–311.
26. Fazilleau, N., L. J. McHeyzer-Williams, H. Rosen, and M. G. McHeyzer-Williams. 2009. The function of follicular helper T cells is regulated by the strength of T cell antigen receptor binding. *Nat. Immunol.* 10: 375–384.
27. Shaffer, A. L., X. Yu, Y. He, J. Boldrick, E. P. Chan, and L. M. Staudt. 2000. BCL-6 represses genes that function in lymphocyte differentiation, inflammation, and cell cycle control. *Immunity* 13: 199–212.
28. Tunyaplin, C., A. L. Shaffer, C. D. Angelin-Duclos, X. Yu, L. M. Staudt, and K. L. Calame. 2004. Direct repression of prdm1 by Bcl-6 inhibits plasmacytic differentiation. *J. Immunol.* 173: 1158–1165.
29. Oracki, S. A., J. A. Walker, M. L. Hibbs, L. M. Corcoran, and D. M. Tarlinton. 2010. Plasma cell development and survival. *Immunol. Rev.* 237: 140–159.
30. Shapiro-Shelef, M., and K. Calame. 2005. Regulation of plasma-cell development. *Nat. Rev. Immunol.* 5: 230–242.
31. Belz, G. T., and A. Kallies. 2010. Effector and memory $CD8^+$ T cell differentiation: toward a molecular understanding of fate determination. *Curr. Opin. Immunol.* 22: 279–285.
32. Crotty, S., R. J. Johnston, and S. P. Schoenberger. 2010. Effectors and memories: Bcl-6 and Blimp-1 in T and B lymphocyte differentiation. *Nat. Immunol.* 11: 114–120.
33. Weber, J. P., F. Fuhrmann, and A. Hutloff. 2012. T-follicular helper cells survive as long-term memory cells. *Eur. J. Immunol.* 42: 1981–1988.
34. Oxenius, A., M. F. Bachmann, R. M. Zinkernagel, and H. Hengartner. 1998. Virus-specific MHC-class II-restricted TCR-transgenic mice: effects on humoral and cellular immune responses after viral infection. *Eur. J. Immunol.* 28: 390–400.
35. Rutishauser, R. L., G. A. Martins, S. Kalachikov, A. Chandele, I. A. Parish, E. Meffre, J. Jacob, K. Calame, and S. M. Kaech. 2009. Transcriptional repressor Blimp-1 promotes $CD8^+$ T cell terminal differentiation and represses the acquisition of central memory T cell properties. *Immunity* 31: 296–308.
36. McCausland, M. M., I. Yusuf, H. Tran, N. Ono, Y. Yanagi, and S. Crotty. 2007. SAP regulation of follicular helper CD4 T cell development and humoral immunity is independent of SLAM and Fyn kinase. *J. Immunol.* 178: 817–828.
37. Gautier, L., L. Cope, B. M. Bolstad, and R. A. Irizarry. 2004. affy—analysis of Affymetrix GeneChip data at the probe level. *Bioinformatics* 20: 307–315.
38. Pavlidis, P., and W. S. Noble. 2003. Matrix2png: a utility for visualizing matrix data. *Bioinformatics* 19: 295–296.
39. Baumjohann, D., T. Okada, and K. M. Ansel. 2011. Cutting edge: distinct waves of BCL6 expression during T follicular helper cell development. *J. Immunol.* 187: 2089–2092.

40. Nurieva, R. I., Y. Chung, D. Hwang, X. O. Yang, H. S. Kang, L. Ma, Y. H. Wang, S. S. Watowich, A. M. Jetten, Q. Tian, and C. Dong. 2008. Generation of T follicular helper cells is mediated by interleukin-21 but independent of T helper 1, 2, or 17 cell lineages. *Immunity* 29: 138–149.
41. Malek, T. R. 2008. The biology of interleukin-2. *Annu. Rev. Immunol.* 26: 453–479.
42. Deenick, E. K., A. Chan, C. S. Ma, D. Gatto, P. L. Schwartzberg, R. Brink, and S. G. Tangye. 2010. Follicular helper T cell differentiation requires continuous antigen presentation that is independent of unique B cell signaling. *Immunity* 33: 241–253.
43. Goenka, R., L. G. Barnett, J. S. Silver, P. J. O'Neill, C. A. Hunter, M. P. Cancro, and T. M. Laufer. 2011. Cutting edge: dendritic cell-restricted antigen presentation initiates the follicular helper T cell program but cannot complete ultimate effector differentiation. *J. Immunol.* 187: 1091–1095.
44. Ploquin, M. J.-Y., U. Eksmond, and G. Kassiotis. 2011. B cells and TCR avidity determine distinct functions of $CD4^+$ T cells in retroviral infection. *J. Immunol.* 187: 3321–3330.
45. Poholek, A. C., K. Hansen, S. G. Hernandez, D. Eto, A. Chandele, J. S. Weinstein, X. Dong, J. M. Odegard, S. M. Kaech, A. L. Dent, et al. 2010. In vivo regulation of Bcl6 and T follicular helper cell development. *J. Immunol.* 185: 313–326.
46. Kaech, S. M., J. T. Tan, E. J. Wherry, B. T. Konieczny, C. D. Surh, and R. Ahmed. 2003. Selective expression of the interleukin 7 receptor identifies effector CD8 T cells that give rise to long-lived memory cells. *Nat. Immunol.* 4: 1191–1198.
47. Marshall, H. D., A. Chandele, Y. W. Jung, H. Meng, A. C. Poholek, I. A. Parish, R. Rutishauser, W. Cui, S. H. Kleinstein, J. Craft, and S. M. Kaech. 2011. Differential expression of Ly6C and T-bet distinguish effector and memory Th1 $CD4^+$ cell properties during viral infection. *Immunity* 35: 633–646.
48. Kalia, V., S. Sarkar, S. Subramaniam, W. N. Haining, K. A. Smith, and R. Ahmed. 2010. Prolonged interleukin-2Rα expression on virus-specific $CD8^+$ T cells favors terminal-effector differentiation in vivo. *Immunity* 32: 91–103.
49. Pipkin, M. E., J. A. Sacks, F. Cruz-Guilloty, M. G. Lichtenheld, M. J. Bevan, and A. Rao. 2010. Interleukin-2 and inflammation induce distinct transcriptional programs that promote the differentiation of effector cytolytic T cells. *Immunity* 32: 79–90.
50. Jeannet, G., C. Boudousquié, N. Gardiol, J. Kang, J. Huelsken, and W. Held. 2010. Essential role of the Wnt pathway effector Tcf-1 for the establishment of functional CD8 T cell memory. *Proc. Natl. Acad. Sci. USA* 107: 9777–9782.
51. Miyazaki, M., R. R. Rivera, K. Miyazaki, Y. C. Lin, Y. Agata, and C. Murre. 2011. The opposing roles of the transcription factor E2A and its antagonist Id3 that orchestrate and enforce the naive fate of T cells. *Nat. Immunol.* 12: 992–1001.
52. Cannarile, M. A., N. A. Lind, R. Rivera, A. D. Sheridan, K. A. Camfield, B. B. Wu, K. P. Cheung, Z. Ding, and A. W. Goldrath. 2006. Transcriptional regulator Id2 mediates $CD8^+$ T cell immunity. *Nat. Immunol.* 7: 1317–1325.
53. Li, J., G. Huston, and S. L. Swain. 2003. IL-7 promotes the transition of CD4 effectors to persistent memory cells. *J. Exp. Med.* 198: 1807–1815.
54. Kondrack, R. M., J. Harbertson, J. T. Tan, M. E. McBreen, C. D. Surh, and L. M. Bradley. 2003. Interleukin 7 regulates the survival and generation of memory CD4 cells. *J. Exp. Med.* 198: 1797–1806.
55. Martins, G. A., L. Cimmino, M. Shapiro-Shelef, M. Szabolcs, A. Herron, E. Magnusdottir, and K. Calame. 2006. Transcriptional repressor Blimp-1 regulates T cell homeostasis and function. *Nat. Immunol.* 7: 457–465.
56. King, C. 2011. A fine romance: T follicular helper cells and B cells. *Immunity* 34: 827–829.
57. Locksley, R. M. 2009. Nine lives: plasticity among T helper cell subsets. *J. Exp. Med.* 206: 1643–1646.
58. Lüthje, K., A. Kallies, Y. Shimohakamada, G. T. T. Belz, A. Light, D. M. Tarlinton, and S. L. Nutt. 2012. The development and fate of follicular helper T cells defined by an IL-21 reporter mouse. *Nat. Immunol.* 13: 491–498.
59. Panzer, M., S. Sitte, S. Wirth, I. Drexler, T. Sparwasser, and D. Voehringer. 2012. Rapid in vivo conversion of effector T cells into Th2 cells during helminth infection. *J. Immunol.* 188: 615–623.
60. Wang, Y.-H., K. S. Voo, B. Liu, C.-Y. Chen, B. Uygungil, W. Spoede, J. A. Bernstein, D. P. Huston, and Y.-J. Liu. 2010. A novel subset of $CD4^+$ T(H)2 memory/effector cells that produce inflammatory IL-17 cytokine and promote the exacerbation of chronic allergic asthma. *J. Exp. Med.* 207: 2479–2491.
61. Hegazy, A. N., M. Peine, C. Helmstetter, I. Panse, A. Fröhlich, A. Bergthaler, L. Flatz, D. D. Pinschewer, A. Radbruch, and M. Löhning. 2010. Interferons direct Th2 cell reprogramming to generate a stable GATA-3^+T-bet^+ cell subset with combined Th2 and Th1 cell functions. *Immunity* 32: 116–128.
62. Mitsdoerffer, M., Y. Lee, A. Jäger, H.-J. Kim, T. Korn, J. K. Kolls, H. Cantor, E. Bettelli, and V. K. Kuchroo. 2010. Proinflammatory T helper type 17 cells are effective B-cell helpers. *Proc. Natl. Acad. Sci. USA* 107: 14292–14297.
63. Watt, F. M., and B. L. Hogan. 2000. Out of Eden: stem cells and their niches. *Science* 287: 1427–1430.
64. Oestreich, K. J., A. C. Huang, and A. S. Weinmann. 2011. The lineage-defining factors T-bet and Bcl-6 collaborate to regulate Th1 gene expression patterns. *J. Exp. Med.* 208: 1001–1013.
65. Kaech, S. M., and R. Ahmed. 2001. Memory $CD8^+$ T cell differentiation: initial antigen encounter triggers a developmental program in naïve cells. *Nat. Immunol.* 2: 415–422.
66. Mercado, R., S. Vijh, S. E. Allen, K. Kerksiek, I. M. Pilip, and E. G. Pamer. 2000. Early programming of T cell populations responding to bacterial infection. *J. Immunol.* 165: 6833-6839.
67. Bajénoff, M., O. Wurtz, and S. Guerder. 2002. Repeated antigen exposure is necessary for the differentiation, but not the initial proliferation, of naive $CD4^+$ T cells. *J. Immunol.* 168: 1723–1729.
68. Yusuf, I., R. Kageyama, L. Monticelli, R. J. Johnston, D. Ditoro, K. Hansen, B. Barnett, and S. Crotty. 2010. Germinal center T follicular helper cell IL-4 production is dependent on signaling lymphocytic activation molecule receptor (CD150). *J. Immunol.* 185: 190–202.
69. Whitmire, J. K., M. S. Asano, S. M. Kaech, S. Sarkar, L. G. Hannum, M. J. Shlomchik, and R. Ahmed. 2009. Requirement of B cells for generating $CD4^+$ T cell memory. *J. Immunol.* 182: 1868–1876.
70. Zhao, D.-M., S. Yu, X. Zhou, J. S. Haring, W. Held, V. P. Badovinac, J. T. Harty, and H.-H. Xue. 2010. Constitutive activation of Wnt signaling favors generation of memory CD8 T cells. *J. Immunol.* 184: 1191–1199.
71. Prlic, M., and M. J. Bevan. 2011. Cutting edge: β-catenin is dispensable for T cell effector differentiation, memory formation, and recall responses. *J. Immunol.* 187: 1542–1546.
72. Engel, I., and C. Murre. 2001. The function of E- and Id proteins in lymphocyte development. *Nat. Rev. Immunol.* 1: 193–199.
73. D'Cruz, L. M., M. P. Rubinstein, and A. W. Goldrath. 2009. Surviving the crash: transitioning from effector to memory $CD8^+$ T cell. *Semin. Immunol.* 21: 92–98.
74. Yang, C. Y., J. A. Best, J. Knell, E. Yang, A. D. Sheridan, A. K. Jesionek, H. S. Li, R. R. Rivera, K. C. Lind, L. M. D'Cruz, et al. 2011. The transcriptional regulators Id2 and Id3 control the formation of distinct memory CD8+ T cell subsets. *Nat. Immunol.* 12: 1221–1229.
75. Ji, Y., Z. Pos, M. Rao, C. A. Klebanoff, Z. Yu, M. Sukumar, R. N. Reger, D. C. Palmer, Z. A. Borman, P. Muranski, et al. 2011. Repression of the DNA-binding inhibitor Id3 by Blimp-1 limits the formation of memory $CD8^+$ T cells. *Nat. Immunol.* 12: 1230–1237.
76. Hand, T. W., M. Morre, and S. M. Kaech. 2007. Expression of IL-7 receptor α is necessary but not sufficient for the formation of memory CD8 T cells during viral infection. *Proc. Natl. Acad. Sci. USA* 104: 11730–11735.
77. Duy, C., C. Hurtz, S. Shojaee, L. Cerchietti, H. Geng, S. Swaminathan, L. Klemm, S. M. Kweon, R. Nahar, M. Braig, et al. 2011. BCL6 enables Ph^+ acute lymphoblastic leukaemia cells to survive BCR-ABL1 kinase inhibition. *Nature* 473: 384–388.
78. Hurtz, C., K. Hatzi, L. Cerchietti, M. Braig, E. Park, Y.-M. Kim, S. Herzog, P. Ramezani-Rad, H. Jumaa, M. C. Müller, et al. 2011. BCL6-mediated repression of p53 is critical for leukemia stem cell survival in chronic myeloid leukemia. *J. Exp. Med.* 208: 2163–2174.
79. Harty, J. T., and V. P. Badovinac. 2008. Shaping and reshaping $CD8^+$ T-cell memory. *Nat. Rev. Immunol.* 8: 107–119.
80. Katz, D. H., W. E. Paul, E. A. Goidl, and B. Benacerraf. 1970. Carrier function in anti-hapten immune responses. I. Enhancement of primary and secondary anti-hapten antibody responses by carrier preimmunization. *J. Exp. Med.* 132: 261–282.
81. Welsh, R. M., L. K. Selin, and E. Szomolanyi-Tsuda. 2004. Immunological memory to viral infections. *Annu. Rev. Immunol.* 22: 711–743.
82. Chevalier, N., D. Jarrossay, E. Ho, D. T. Avery, C. S. Ma, D. Yu, F. Sallusto, S. G. Tangye, and C. R. Mackay. 2011. CXCR5 expressing human central memory CD4 T cells and their relevance for humoral immune responses. *J. Immunol.* 186: 5556–5568.
83. Bossaller, L., J. Burger, R. Draeger, B. Grimbacher, R. Knoth, A. Plebani, A. Durandy, U. Baumann, M. Schlesier, A. A. Welcher, et al. 2006. ICOS deficiency is associated with a severe reduction of $CXCR5^+$ CD4 germinal center Th cells. *J. Immunol.* 177: 4927–4932.